Mechanisms of Stability and Energy Expenditure in Human Locomotion

by

John R Rebula

A dissertation submitted in partial fulfillment
of the requirements for the degree of
Doctor of Philosophy
(Mechanical Engineering)
in the University of Michigan
2014

Doctoral Committee:

Professor Arthur D. Kuo, Chair
Professor Ryan M. Eustice
Professor Noel C. Perkins
Professor Kathleen H. Sienko

2014

Many colleagues have helped with this work over the years, so thanks!

TABLE OF CONTENTS

LIST OF FIGURES

LIST OF TABLES

ABSTRACT

Mechanisms of Stability and Energy Expenditure in Human Locomotion
by John R Rebula

Chair: Arthur D. Kuo

Although humans normally walk with both stability and energy economy, either feature may be challenging for persons with disabilities. For example, in patients with lower-limb amputation, falling is pervasive, and may lead to activity avoidance. Similarly, energy expenditure is higher than for healthy subjects and may deter patients from walking, reducing mobility. A better understanding of the fundamental principles of stability and economy could lead to better prostheses that increase quality of life for patients. When designing a mechanism to assist or mimic human gait, such as orthoses or walking robots, the stability and economy of the resulting gait should be considered. To further our understanding of these fundamental principles of gait, I explore a lesser known balance mechanism, foot heading, as well as the role of muscle force production costs in gait. To investigate the role of foot heading in stabilizing gait, I first characterize a method of measuring natural human gait variability outside of lab environments using foot mounted inertial sensors. Accuracy is found comparable to motion capture, while allowing capture of gait in natural environments. Then, using both a simple model of walking, and a variability analysis of walking in humans, I present evidence that humans stabilize gait laterally by altering foot heading step-to-step. I then consider the metabolic cost of force production in human locomotion. First, an optimization study of a simple model of locomotion shows that force fluctuation costs have a stronger role in determining gait than force amplitude costs. I then illustrate the connection between force fluctuation and a cost for calcium pumping in muscles using a simple muscle model. Finally, a human subject experiment altering force fluctuation in walking demonstrates the higher metabolic cost of fluctuating forces. While human locomotion is a complex activity involving many muscles, sensory systems, and neural circuitry, we are able to learn about the underlying principles of gait using basic mechanical models. A better understanding of stability and economy could have applications to many fields involving locomotion, such as the diagnosis of fall-risk in elderly subjects, the development of rehabilitation techniques, the design of prostheses, and the creation of robust and practical walking machines.

CHAPTER 1

Introduction

Humans appear to locomote in ways that avoid both injury and unnecessary energy expenditure. One way humans may avoid injury is by walking in a stable manner, which is unlikely to result in a fall. Likewise, a human may choose to walk economically, walking a given distance in a manner that reduces energy expended (measured, for example, in calories consumed). Healthy humans locomote with fairly robust stability and economy, but these qualities often suffer in other forms of locomotion, such as robotic walking. In addition, a subject using an engineered lower limb prosthesis generally suffers from adverse energy economy and increased fall risk. This work is part of a broad effort to better characterize mechanisms of stability and energetic economy in bipedal gait in general. A better understanding of stability and economy could have potential applications to the diagnosis of fall-risk in elderly subjects, the development of better rehabilitation techniques, the design of better prostheses, and the creation of more robust and practical walking machines.

While human locomotion is a complex activity involving many muscles, sensory systems, and neural circuitry, there may be underlying principles governing gait based on the mechanics of walking. For example, a simple *passive dynamic walker* consisting of two rigid links, representing legs, joined by a hinge joint, representing the hip, can walk down a slope if started in the right configuration [60]. If actuation is added such that the walker can exert a pushoff force when the trailing foot leaves the ground (toeoff), this *dynamic walker* can walk on flat ground [53]. These models are described as *dynamic* because they rely on their motion to avoid falling. For example, if the hip hinge joint is locked during a step, the walker may fall. This is in contrast to a very slow gait where the system is kept statically stable at all times, and locking the joints would result in standing still. We model human locomotion using dynamic walkers because, except for very slow walking, human gait is also dynamic. Analysis of the powered dynamic walker described above allows researchers to study the energetic consequences of powering gait using pushoff. Simple dynamic walkers allow straightforward calculation of the mechanical power required to walk at a given speed, and can be used to predict the effect of reducing pushoff, as in the case of a lower leg

amputation. Such models allow the isolated study of properties of gait, independent of the particulars of a given model of muscles or joints. The results from such studies are easily interpretable and are not dependent on the correct choice of a large number of parameters, such as when modelling muscles. Furthermore, model results that do not depend on the details of human anatomy and can also be applied equally to artificial walking machines. Therefore, in order to study stability and energetics, this work will use a combination of simple modeled walking, which allows isolated and easily interpretable experimentation, as well as healthy human walking, which provides an example of stable and efficient gait.

This work is divided into two main parts. First is an analysis of the use of foot heading (*steering*) as a mechanism of stabilizing natural gait, second is an analysis of the cost of producing leg forces in gait. Each of these parts adds to our knowledge of general legged locomotion by exploring stability or energy efficiency using both simple walking models and experimental observation of human walking.

The first study (Chapter 2) characterizes a method of measuring human gait variability outside of lab environments using foot mounted inertial sensors. Typical gait measurement occurs in a laboratory environment (e.g. [6]). This has the advantage of allowing careful control of experimental conditions, and also allows the use of laboratory based measurement techniques such as motion capture, pressure sensitive mats, and speed controlled treadmills (e.g. [67]). Walking stability, for example, can be characterized based on variability of walking [13]. However, measuring gait variability accurately can require a large number of measured steps. It is straightforward to measure many contiguous steps on a treadmill, but treadmill walking generally imposes constraints (speed, lateral motion) as well as sensory differences (visual flow) that could limit the applicability of treadmill studies [73]. Furthermore, laboratory walking does not necessarily represent how the subject walks outside of the lab. Therefore, we develop a method of estimating the trajectories of the feet during walking from unobtrusive foot-mounted inertial sensors. This allows estimation of foot placement, orientation, and their variabilities, even if walking in natural terrain. Accuracy was found comparable to motion capture. Using this method, commercially available inertial sensors can be used to unobtrusively capture foot trajectories for essentially a full day. This provides a new method of measuring human activity in natural environments, providing richer data than standard accelerometry or step counting.

The second study (Chapter 3) is an analysis of the role of foot heading to stabilize bipedal walking. The role of foot heading is explored in two ways. First, a 3-dimensional walking model is presented which walks passively down a gentle slope. This passive gait is stable in the fore-aft direction. If it is pushed a small amount forward or backward, it will recover and converge back to the passive gait with no control actuation required. However,

it is unstable in the lateral direction, and any lateral disturbance will result in an eventual fall. Actively controlling lateral foot placement is one way to stabilize this unstable lateral mode [49]. Here, the model is extended to allow a yaw rotation of the pelvis with respect to the stance foot, which alters the heading of the walker. We perform a stability analysis of the linearized controlled walking system treating yaw rotation as a control input. We find that foot heading can stabilize the walking gait in a manner similar to lateral foot placement. That is, when disturbed to the right, a stabilizing controller would both move the swing foot more to the right than normal, and rotate the body to point more to the right.

Another method I use to explore the role of foot heading in stabilizing bipedal walking is an observational study of overground human walking. The inertial measurement technique described above (Chapter 2) is used to measure subjects walking down a straight hallway for many steps (about 90). Since walking is laterally unstable, any deviations in lateral foot placement are treated as indications of small corrections in lateral stability. I therefore look for a correlation between lateral foot placement and foot heading angle. A sensitivity of 0.38 radians/m is found between foot heading and stride width, suggesting that both foot placement and steering are used to balance laterally. This finding suggests that even in normal, unperturbed walking, small corrections to balance are being made on a step to step basis, and analysis of a large number of overground steps can reveal these relationships.

The remainder of this work is an exploration of the cost of force production in human locomotion. The manner in which people walk is due, in part, to the fundamental energetic costs associated with human motion [90]. In order to operate, natural muscle expends chemical energy, which must be supplied by caloric intake. Muscles expend energy to perform useful mechanical work, but they also require energy to activate and maintain force [9]. Here we investigate the tradeoffs between the fundamental costs of mechanical work and force production in the context of human walking. This tradeoff is explored in two ways: first, a computational model based study where the effects of force production can be isolated, and second, a human experiment where subjects walk using specified force profiles, allowing measurement of the effect of force production on actual metabolic cost.

We present an optimization study of a simple model of locomotion to explore the tradeoff between the costs for mechanical work and force production (Chapter 4). Previous optimization studies of modeled locomotion suggest that, if mechanical work is the only cost in walking, the legs should act as perfectly rigid pendulums, with ideal instantaneous forces at heelstrike (impact) and toeoff (pushoff) [83]. This work-optimal gait approximates the inverted pendulum model of walking, which has been used classically as a model of human walking. The inverted pendulum model provides insights into the role of pushoff

in the human ankle and prosthesis design, when there is no longer a natural ankle to provide pushoff force. Here we extend previous optimization studies, and consider costs for both mechanical work and force production. Several forms for the cost of producing force are considered, including costs for force amplitude, as well as costs for fluctuating forces. We find that optimizing for a combination of mechanical work and force amplitude does not produce force profiles resembling human gait. Optimization of a combination of mechanical work and force fluctuation, instead of force amplitude, does discover a qualitatively human-like gait. These findings suggest force fluctuation costs have a stronger role in determining gait than force amplitude costs.

To further explore the cost of fluctuating forces, a simple model of a single muscle producing various force profiles is analyzed (Chapter 5). One possible explanation for a force fluctuation cost is the calcium pumping associated with activating and deactivating muscles. This metabolic cost for calcium pumping in muscles accounts for up to 30% of the total cost for an isometric force twitch [7]. However, in the context of walking, the relationship between this cost and the overall force exerted on the body is not straightforward to quantify, since walking forces involve more than simple isolated twitches. Therefore, I present a simplified model of muscle contraction and activation dynamics taken from the literature, and test the energetic consequences of producing various force profiles with differing levels of force fluctuation. This model shows that force profiles with large fluctuations, but comparable magnitudes, require more calcium pumping to achieve, and therefore have higher metabolic costs. Calcium pumping is therefore considered a possible cause of a cost for force fluctuation.

Finally, to test the metabolic consequences of force fluctuation, a human subject experiment is performed with subjects walking both normally and with altered force fluctuation. Subjects walked on a treadmill with visual feedback of their ground contact via forceplates in the treadmill and a projected display. Differing feedback and instructions resulted in *spikey* walking with larger force fluctuations, similar to inverted pendulum walking, and *smooth* walking with less force fluctuation. These conditions were compared with a control condition, where the subject walked with their preferred ground reaction forces. Subjects expended more metabolic power during both the smooth and spikey walking conditions than the control condition. Furthermore subjects exerted more mechanical power in the smooth condition, and less mechanical power in the spikey condition. These results support the hypothesis that normal human walking involves a tradeoff between the metabolic costs of force fluctuation and mechanical work. This study shows a connection between fundamental costs (in this case for human muscle) and larger aspects of gait, such as the double support period. Walking systems with similar morphology to humans, but with dif-

ferent low level costs (such as a humanoid robot with electric or hydraulic actuators) might have corresponding optimal gaits that look significantly different from human gaits.

CHAPTER 2

Measurement of Foot Placement and its Variability with Inertial Sensors

Gait parameters such as stride length, width, and period, as well as their respective variabilities, are widely used as indicators of mobility and walking function. Foot placement and its variability have thus been applied in areas such as aging, fall risk, spinal cord injury, diabetic neuropathy, and neurological conditions. But a drawback is that these measures are presently best obtained with specialized laboratory equipment such as motion capture systems and instrumented walkways, which may not be available in many clinics and certainly not during daily activities. One alternative is to fix Inertial Measurement Units (IMUs) to the feet or body to gather motion data. However, few existing methods measure foot placement directly, due to drift associated with inertial data. We developed a method to measure stride-to-stride foot placement in unconstrained environments, and tested whether it can accurately quantify gait parameters over long walking distances. The method uses ground contact conditions to correct for drift, and state estimation algorithms to improve estimation of angular orientation. We tested the method with healthy adults walking over-ground, averaging 93 steps per trial, using a mobile motion capture system to provide reference data. We found IMU estimates of mean stride length and duration within 1% of motion capture, and standard deviations of length and width within 4% of motion capture. Step width cannot be directly estimated by IMUs, although lateral stride variability can. Inertial sensors measure walks over arbitrary distances, yielding estimates with good statistical confidence. Gait can thus be measured in a variety of environments, and even applied to long-term monitoring of everyday walking.

2.1 Introduction

Human walking exhibits variability from step to step. This may reflect variations in the sensory, neural, and biomechanical systems that produce gait. Gait parameters such as step length, width, and period and their respective variabilities can therefore serve as indicators of mobility or function in a variety of populations [8,30]. Changes in such parameters have been observed with aging [70] or development [37]. They may be associated with risk or fear of falling [14, 56], cognitive or attentional capacity [21, 36], and brain activity [79]. Step parameters also vary with conditions such as spinal cord injury [22], Parkinson's disease [16], traumatic brain injury [44], cerebellar ataxia [78], and multiple sclerosis [81]. But a difficulty is that the measurement of foot placement typically requires specialized equipment such as motion capture systems, thereby limiting measurements to the laboratory. Technological developments in miniature inertial measurement units (IMUs: accelerometers and gyroscopes) offer the potential to measure strides outside the laboratory. However, accelerometers measure translational accelerations and gyroscopes measure angular velocities in a body-fixed reference frame, and these imperfect measurements must somehow be transformed into foot placement in an absolute frame. If that transformation could be achieved with accuracy comparable to laboratory equipment, it would enable evaluation of strides and stride variability in the field, using only foot-mounted sensors.

One approach for using foot-mounted sensors exploits empirical or kinematic associations between inertial measurements and step parameters. Human walking is quite systematic, so that speed and step parameters are correlated with each other [37] and with inertial measurements. These correlations, derived from previous gait data, allow step parameters to be estimated from IMUs mounted on the body [30, 54, 101]. Estimation accuracy can be improved by calibrating trends for specific individuals [5] rather than a population. This approach is, however, less applicable to gait pathologies or other cases where locomotion may vary considerably from previous calibration data. An alternative is to use a kinematic leg model to associate data from inertial sensors on the leg with step parameters [80, 98]. This also requires kinematic model parameters, which may themselves require calibration for a subject.

Another approach is to integrate inertial measurement data over time to yield positions in space. The principal challenge of integration is drift, referring to errors in position and orientation that accumulate over time due to imperfect data. Drift in orientation may be reduced with a state estimator or Kalman Filter [17], which models the IMU motion in space to predict accelerations and angular velocities, and uses the mismatch with actual measurements to reduce orientation errors. Position drift can be reduced by resetting the

foot's velocity to zero at each footfall. This model assumption is imperfect, but does not rely on subject-specific calibration or normative correlation data. A combination of such drift correction methods can be used to localize the foot in the sagittal plane [75] or in space [31, 58, 68, 77]. Similar assumptions may be applied to waist-mounted IMUs for estimating stride parameters [47]. These methods require minimal assumptions regarding the subject's gait, mainly that the foot is periodically stationary on the ground.

These drift reduction methods may facilitate measurement of foot placement variability over long distances of over-ground walking. Variability is best measured over many strides [71], which is often challenging to capture in absolute space. But stride variability only requires the foot's displacement relative to the preceding footfall, for which drift error can be stabilized using the methods above (e.g., [68]). In the present study, we propose an algorithm, using no skeleton or correlation model, for estimating foot placement and its variability from inertial data. We then test the algorithm against reference data obtained from a mobile motion capture system [69], during long walking bouts.

2.2 Inertial Sensor Processing

We assemble an algorithm to integrate foot-mounted IMU data and yield drift-reduced stride displacements. We divide the processing into four steps (Figure 2.1): (1) stride segmentation, (2) rotational orientation estimation, (3) translational velocity estimation, and (4) trajectory formation. Stride segmentation uses raw sensor measurements to detect zero velocity instants when the foot is stationary on the ground. We estimate orientation by integrating the gyroscope data and correcting for tilt drift with a Kalman Filter. We estimate translational velocity by integrating accelerometer data, then adjusting the velocities to be compatible with each zero velocity instant. Finally, the foot trajectory is formed by integrating the corrected velocities, oriented with respect to a local walking heading. That trajectory directly yields foot placement, from which stride parameters are calculated.

2.2.1 Stride Segmentation

We identify zero velocity instants based on raw IMU data (Figure 2.2 A). We use thresholds on the magnitude of the gyroscope and accelerometer signals to identify these times. Assuming solid ground and no foot slip, the foot velocity and acceleration will be near zero during part of each stance phase. We identify stationary phases as periods when the gyroscope output magnitude is small and the accelerometer output magnitude is close to gravitational (g). The midpoint of each stationary interval defines a zero velocity instant,

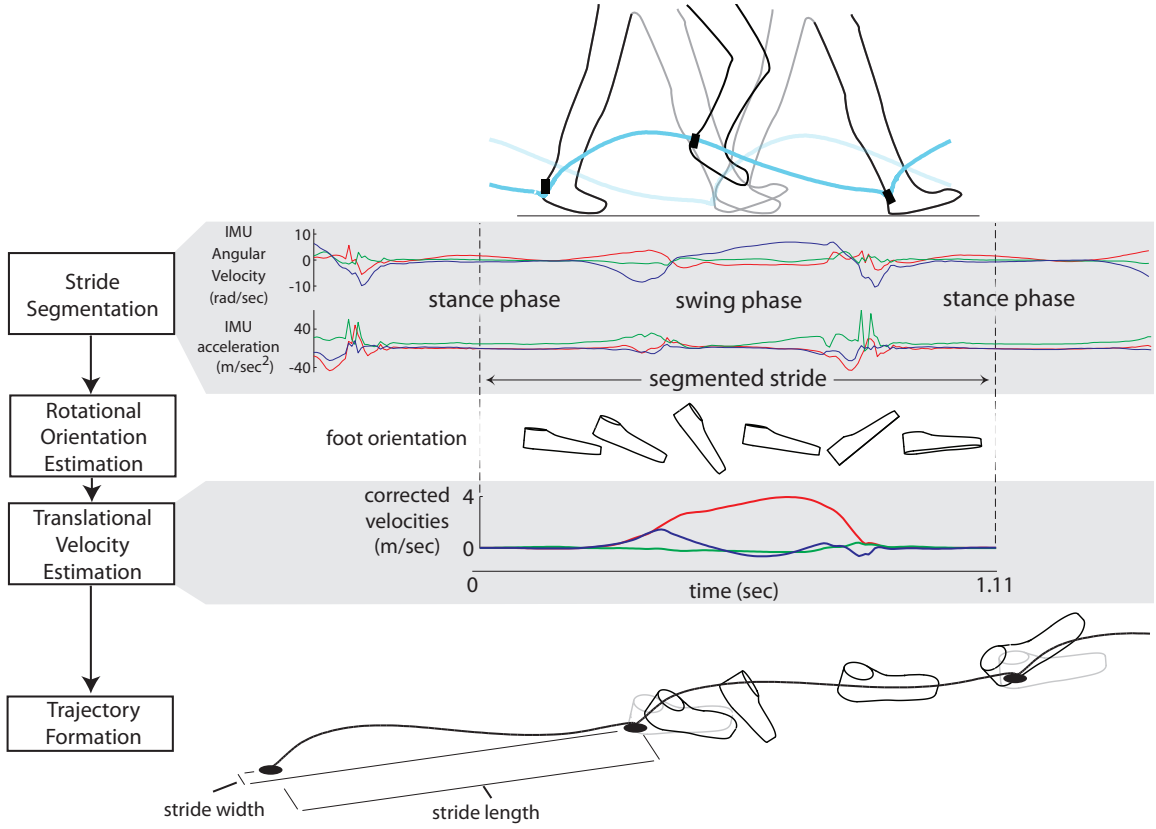

Figure 2.1: Overview of inertial sensor processesing steps. IMU processesing (shown at left), with representative data trajectories (plotted at right). Stride segmentation uses accelerometer and gyroscope readings to determine periods when the foot is stationary on the ground. Orientation estimation uses a Kalman Filter to correct for drift in tilt and yield orientation of the foot in space. Velocity estimation is performed by integrating tilt-corrected accelerometer signals, subject to a zero velocity correction. Finally, trajectory formation is performed by integrating corrected velocities to yield foot trajectories in space.

demarcating strides. In the present study, we used magnitude thresholds of 1.7 radian$\cdot$s^{-1} and 0.8 m$\cdot$s^{-2} (relative to g). We also exclude erroneously detected phases caused by short periods of constant velocity and low angular velocity during swing, as well as quick foot slips during stance. These are detected as unusually short stationary or swing periods. We have found minimum period thresholds of 0.133 s for stationary and 0.2 s for swing to perform well.

This simple algorithm identifies zero velocity instants during normal walking using few parameters. It is not optimized for estimating stance and swing durations nor for detecting events such as footfall or toe-off.

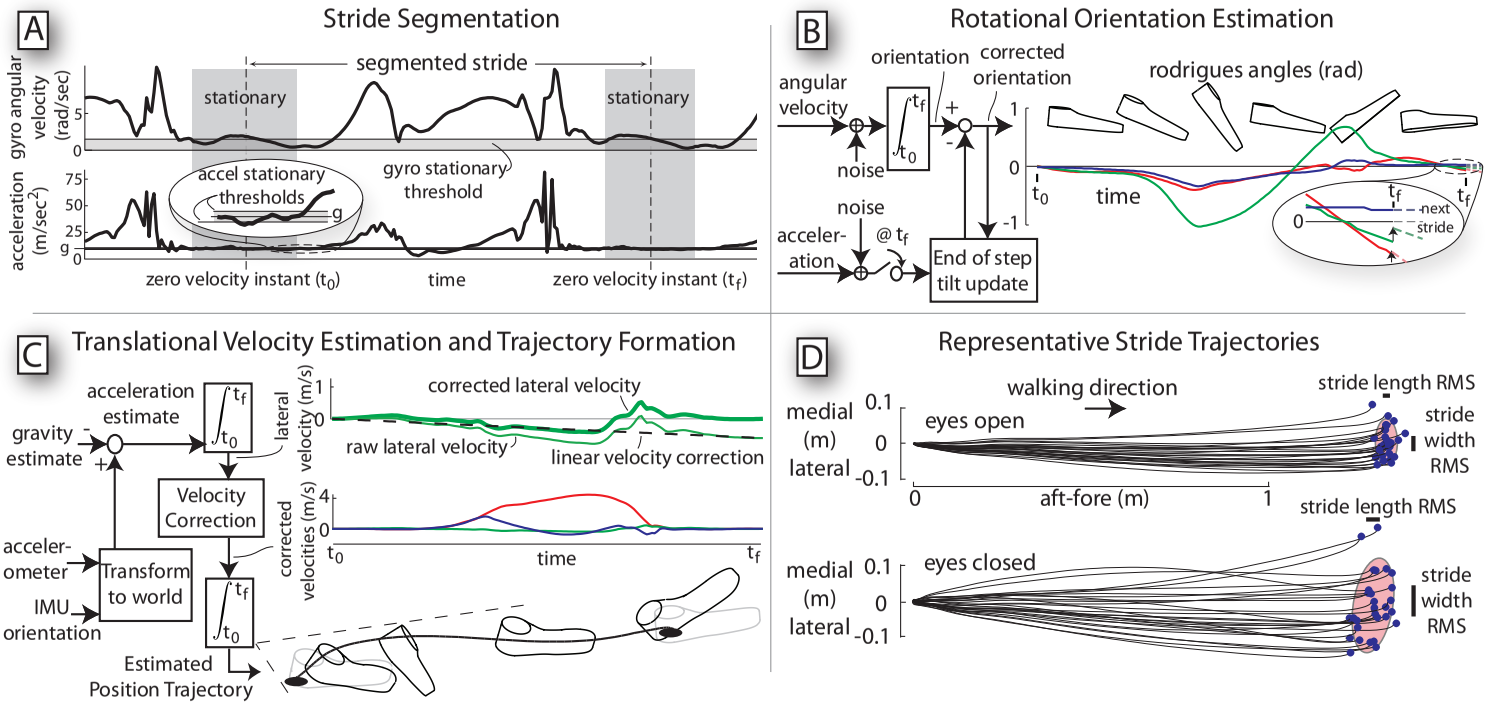

Figure 2.2: Detailed inertial sensor processing. **A:** Stride segmentation to determine stationary foot instants. Thresholds on the magnitudes of the gyroscope (top) and accelerometer (bottom) signals determine foot stationary phases. A minimum phase duration is used to reduce the effect of noise. The midpoint of each stationary phase defines a zero velocity instant, demarcating strides. **B:** Orientation estimation algorithm. Orientation of the foot is estimated by integrating angular velocities from foot-mounted gyroscopes. At each zero velocity instant during stance ($t = t_f$), the accelerometer provides an estimate of gravity, which is used to perform a discrete Kalman update of the orientation estimate. The orientation trajectories (plotted as Rodrigues angles) are corrected impulsively at the end of each stride (inset). **C:** Velocity estimation and trajectory formation. Translational velocity is found by integrating the transformed and gravity compensated accelerometer readings during the stride. A zero velocity correction is then applied, where a linear trend is subtracted from the cumulative velocity between stationary instants. Finally, the trajectory of the foot is found by integrating the velocity, and stride parameters are then calculated from the trajectories. **D:** Foot trajectories and stride measurements from IMU data. Overhead view is shown of representative IMU trajectories for the right foot of one subject, for an eyes open (top) and eyes closed (bottom) walking trial. The trajectories are aligned to a common origin at the beginning of each stride. Stride length and width are defined by a local heading determined from three successive strides. Stride variability is defined as the root-mean-square (RMS) variability of length and width.

2.2.2 Rotational Orientation estimation

Orientation of each IMU in space is determined by integrating gyroscope signals with a discrete Kalman Filter (Figure 2.2 B). Gyroscope-derived orientations are subject to drift, but the estimated vertical direction, referred to as tilt, can be corrected based on the accelerometer's reading of gravity. We integrate the gyroscope signals over time to estimate the 3d angular orientation of the IMU [68]. Then a discrete tilt correction is applied at the detected zero velocity instant at the end of each stride. The accelerometers are used as an inclinometer to produce a discrete Kalman update, which stabilizes tilt drift over arbitrarily long durations. The Kalman Filter requires relative values of the measurement and process noise to integrate the sensors. The gyroscope variance describes the gyroscope noise, the accelerometer variance describes the accelerometer noise and the zero velocity assumption noise. The process variance describes the constant angular velocity assumption noise. We found modest gains sufficient for tilt correction, with the Kalman updates correcting about $2.6 \cdot 10^{-3}$ tilt radians per footfall.

The integration yields a time-varying representation of the IMU's orientation. This is expressed relative to the IMU's initial orientation, which is an arbitrary home orientation reference (the IMU can be attached to the foot in any orientation). The gravity vector in the initial orientation defines vertical. The output of these calculations is therefore a tilt-corrected IMU orientation in space. This algorithm does not correct for drift in heading about vertical, which can potentially be reduced using other sensors such as magnetometers [31].

2.2.3 Translational Velocity estimation

Foot velocity can be estimated from accelerometer signals (Figure 2.2 C). We first use the IMU orientation to transform accelerometer readings into absolute space. Acceleration in space is found by subtracting the estimated gravity vector. The result is integrated forward in time, starting at one detected zero velocity instant and ending at the next. This yields a velocity estimate which is subject to drift during each stride. To correct for drift, we constrain foot velocity to zero at the zero velocity instant at the end of each stride. Rather than an impulsive correction [68], we distribute the correction over the stride assuming that error grows linearly with time, to yield a smooth correction.

2.2.4 Trajectory formation

The foot's trajectory in space is obtained by integrating the corrected velocities (Figure 2.2 C). This is also subject to unbounded drift in absolute space, but stride measurement only requires displacement relative to the preceding footfall. Foot placement therefore only drifts over the relatively short duration of a single stride, and can be estimated with reasonable accuracy. It is obtained by integrating foot velocity between successive zero velocity instants. Having corrected for drift in tilt and foot placement, the resulting trajectory is mostly only subject to growing drift in heading about vertical. Since subjects may also vary heading anyway, we do not rely on the global heading estimate over long durations.

To measure stride displacements, we define a local heading from foot trajectories. We define the forward walking direction from a linear fit of three successive footfalls locations. The forward direction and gravity vector together define the local lateral direction. Each foot trajectory is then examined with respect to the local frame (Figure 2.2 D).

Finally, we compute stride parameters (Figure 2.2 D). Stride parameters, such as stride length and width, are calculated from the foot trajectories between successive footfalls in their local frames. Stride variability is computed from the root-mean-square variations about the average stride length and width. Stride duration is calculated based on the difference between successive peak times of filtered estimated speed. All integrations are performed using the trapezoidal method.

2.3 Experiment

We tested IMU-based stride measurements against motion capture performed during overground walking. We measured 9 healthy young subjects walking normally with eyes open, and induced greater variability by collecting trials with eyes closed. This is intended to test the sensitivity of stride measurements to changes that might occur with a gait pathology. We used a cart-mounted motion capture system to collect simultaneous reference data (Figure 2.3). We quantified both the statistical agreement between the IMU and motion capture estimates, and the sensitivity of the IMU and motion capture estimates to different walking conditions. Subjects provided informed consent according to Institutional Review Board procedures.

Each subject performed multiple straight walking trials down a hallway. An average of 93 steps were recorded per trial, and a total of 90 trials were collected of both conditions. An IMU was attached to the heel of each shoe (Memsense, Rapid City, South Dakota, nIMUs, gyroscope range: $1200deg \cdot s^{-1}$, accelerometer range: $10g$, sampled at 150 Hz).

To provide a laboratory-based measurement of foot kinematics, a motion capture system (PhaseSpace, Inc. San Leandro, California) with six cameras was mounted on a mobile cart. The cart was equipped with a vertical axis gyroscope and two wheel encoders to localize the cart using dead reckoning [69]. The subject stood motionless for 20 seconds prior to each trial to yield baseline inertial sensor data. A total of 22 trials were excluded due to hardware failures or protocol deviations. Within each trial, the first and last 6 steps were excluded to focus on steady walking. During eyes closed trials, two experimenters walked beside the subject and provided audible cues to keep the subject near the centerline of the hallway.

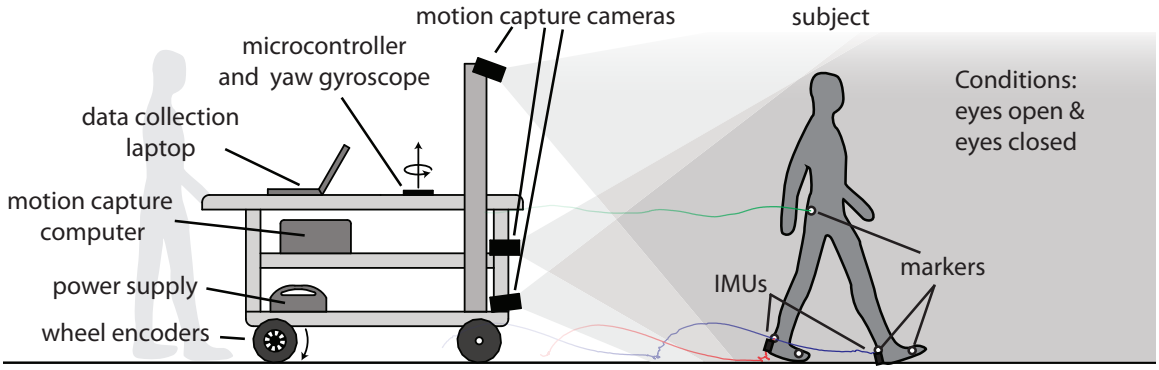

Figure 2.3: Experimental setup for testing foot placement measurement. Subjects walked down a hallway while wearing foot-mounted IMUs and motion capture markers. To collect reference data, an experimenter pushed a mobile motion capture cart behind the subject. The cart was instrumented to use dead reckoning to calculate the motion of the subject in a world frame, yielding a comparison between motion capture and IMU results.

We examined the agreement between the IMU and motion capture stride estimates. To test the performance of the IMU estimation, we compared the IMU-based stride estimates against motion capture. This was performed for eyes open and eyes closed conditions to test sensititivity to changes in gait. Because neither measurement is perfectly accurate, we compared motion capture and IMU stride estimates using intraclass correlation (ICC), which summarizes the agreement between methods and quantifies unexplained variance in the data ([61]; A-1 method). We summarized gait variability for stride length, width, and duration by calculating root mean squares (RMS) for each walk, and averaging across walks for each condition for each subject. To compare the sensitivity of IMU estimates to motion capture estimates, we performed a paired t-test between eyes closed and eyes open estimates.

2.4 Results

We found the IMU estimates of gait parameters to agree reasonably well with motion capture data (Figure 2.4 A). Estimates of mean stride parameters agreed to within 1%, and estimates of RMS variability of stride width and length agreed to within 4%. (Estimates of stride duration variability agreed less well; we believe this is due to poor motion capture estimates.) As an indicator of the ability to detect relatively subtle changes to gait, both methods revealed significant increases in stride width and length variability for walking with eyes closed. No significant difference was observed in other measures for eyes closed walking, using either measurement method. We summarize the overall correspondence between IMU and motion capture in two ways. First, the RMS difference between the IMU and motion capture estimates of all stride lengths is 3.2% of the mean stride length. Second, we quantify the fraction of data variation shared by the two instruments using the intra-class correlation coefficient (ICC). We observed ICC values of 0.88 for stride width, and 0.98 for stride length (Figure 2.4 B), indicating good agreement.

2.5 Discussion

We sought to determine whether foot-mounted IMUs can estimate stride measures from over-ground walking. We devised an algorithm that calculates stride parameters that are drift-stabilized, meaning that errors do not grow unbounded with time. Results show that stride measures are comparable between IMU and motion capture methods (Figure 2.4 A), agreeing to within a few percent. Both methods also agree on increased stride variability resulting from walking with eyes closed, indicating sufficient sensitivity to detect relatively small changes in gait [8]. Having quantified IMU performance relative to motion capture, we next consider the limitations and provide recommendations for use.

The main sensitivity of this algorithm is to stride segmentation. Stride segmentation errors, when a stationary instant fails to be detected, or when one is detected during the swing phase, significantly degrade the algorithm's performance. Such errors are normally not an issue except during extremely slow or unsteady walking. Stride segmentation may be facilitated through good sensor placement. Here we used the back of the shoe to accommodate comparison with motion capture, but we prefer the top of the shoe above the instep, which yields longer stationarity durations. The segmentation algorithm can also be improved by applying additional constraints. If both feet are instrumented with time-synchronized IMUs, the swing of one foot can indicate stationarity of the other. This can reduce segmentation errors substantially, albeit only for walking and not running gaits. The

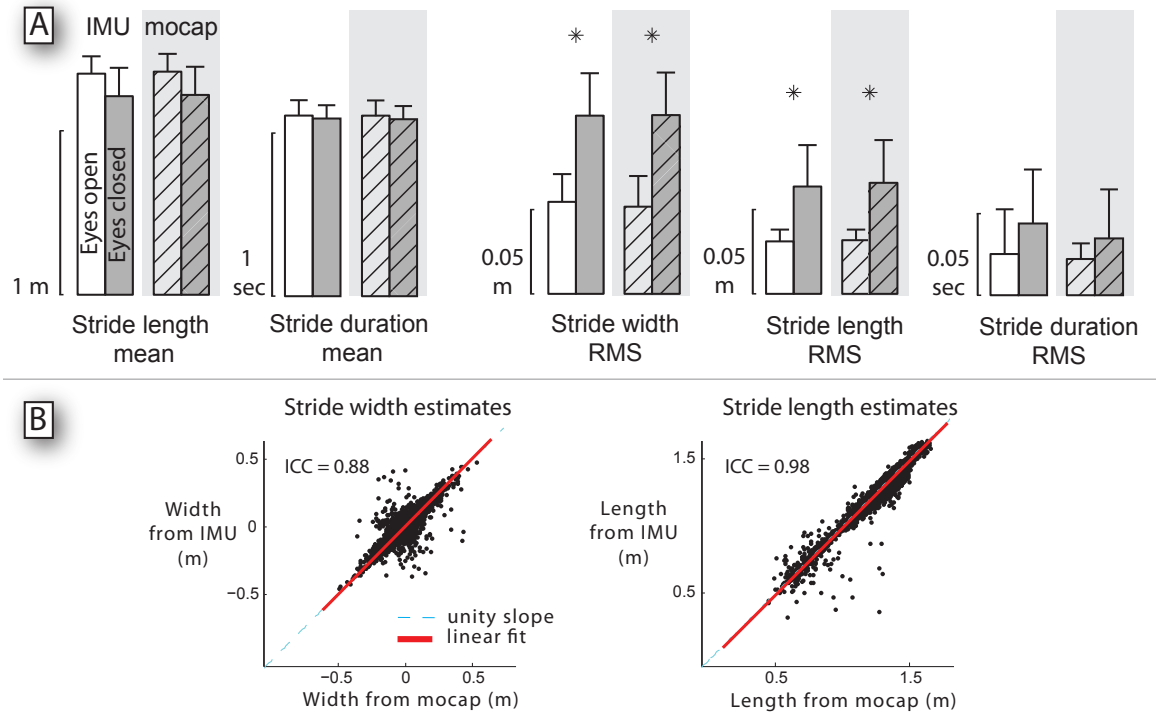

Figure 2.4: Comparison of stride parameters as measured with IMU and motion capture. **A:** Shown are mean stride length and duration, and RMS variability of stride width, length and duration, for eyes open and eyes closed conditions. Error bars represent standard deviation across subjects. Asterisks denote significant differences detected between eyes open and closed conditions (paired t-test, $p < 0.05$). **B:** Correlation between stride measurements using IMU and motion capture. Individual stride width and length estimates are shown for all subjects and conditions (5538 strides). IMU estimates are plotted against motion capture estimates, along with intra-class correlation (ICC) and the corresponding linear fit. Perfect agreement would yield a line of unity slope.

algorithm presented here is simple and uses few parameters; it can easily be replaced by alternative methods as appropriate.

There are a few assumptions under which the proposed algorithm performs best. One is that drift in translational velocity occurs continuously over time. We distribute each stride's velocity correction (Figure 2.2 C) linearly over the entire time interval between stationary instants. Alternately, the velocity could be corrected impulsively, for example at each stationary instant [68]. This may be appropriate if the errors occur at that time, such as with gyroscopes that are sensitive to the impulsive accelerations of heelstrike. Another assumption is that foot motions are within the IMU's range and bandwidth. To estimate the consequences of these assumptions, we reprocessed our data with impulsive velocity corrections, and separately with artificially reduced sensor ranges (Figure 2.5 A). We found

the distributed velocity correction to yield considerably lower errors (with respect to motion capture) compared with impulsive correction. We also found a sharp performance degradation when limiting IMU ranges. Decreasing the gyroscope range resulted in stride length estimate outliers similar to the strides with uncharacteristically low length estimates from the IMU (Figure 2.4 B). Therefore a likely cause for these outliers is momentary gyroscope saturation. Our algorithm appears to work best with distributed zero correction, and with IMUs with sufficient ranges and bandwidth.

Although not the focus of this study, integration methods such as ours are also applicable to position estimation in space. Previous studies based on integration of inertial data have measured relatively short walking bouts [31, 68]. Our methods can also track an IMU reasonably well in space for distances on the order of 100 m (Figure 2.5 B). Most integration methods rely on the principal assumption of a zero velocity instant within each stride, reducing but not eliminating drift. Further drift reduction is possible using additional assumptions. For example, if the walking surface is assumed level, altitude drift can be reduced. If the heading is constant [11], or measurable with magnetometers or GPS [31], its drift can also be reduced. Position, velocity, and sensor calibrations can be incorporated into the Kalman Filter in addition to the proposed Kalman filtering scheme, allowing zero velocity updates to correct angular orientation estimates [31]. A spline based velocity correction can also be used to correct foot velocity, which works well in certain circumstances with sensors of limited range [58]. Of course, such variations require additional assumptions, which can lead to amplified errors if violated. For general applicability, we have presented a near-minimal set of assumptions here.

Integration methods complement other gait measurement methods. These include IMU approaches using a kinematic body model or a correlation model from walking data. These may be accurate under particular conditions, but may become inaccurate when the models do not apply. In contrast, integration methods assume nothing of the human's geometry or motion other than the existence of zero velocity instants. They also apply to relatively unconstrained, over-ground locomotion in varied environments. This contrasts with laboratory measurements using motion capture or sensor-embedded walkways. These can yield accurate drift-free measurements, but usually for a limited number of steps in a confined space. An advantage of IMU integration is that a large number of strides may be measured with good accuracy. This can enhance stride parameter estimation (e.g., [71]). An example is the effect of walking with eyes open versus closed, which is best discriminated with a relatively large number of strides (Figure 2.5 C), which are otherwise difficult to capture accurately during over-ground walking. Given accurate inertial sensors, we believe integration methods are especially well suited for the estimation of stride parameters and their

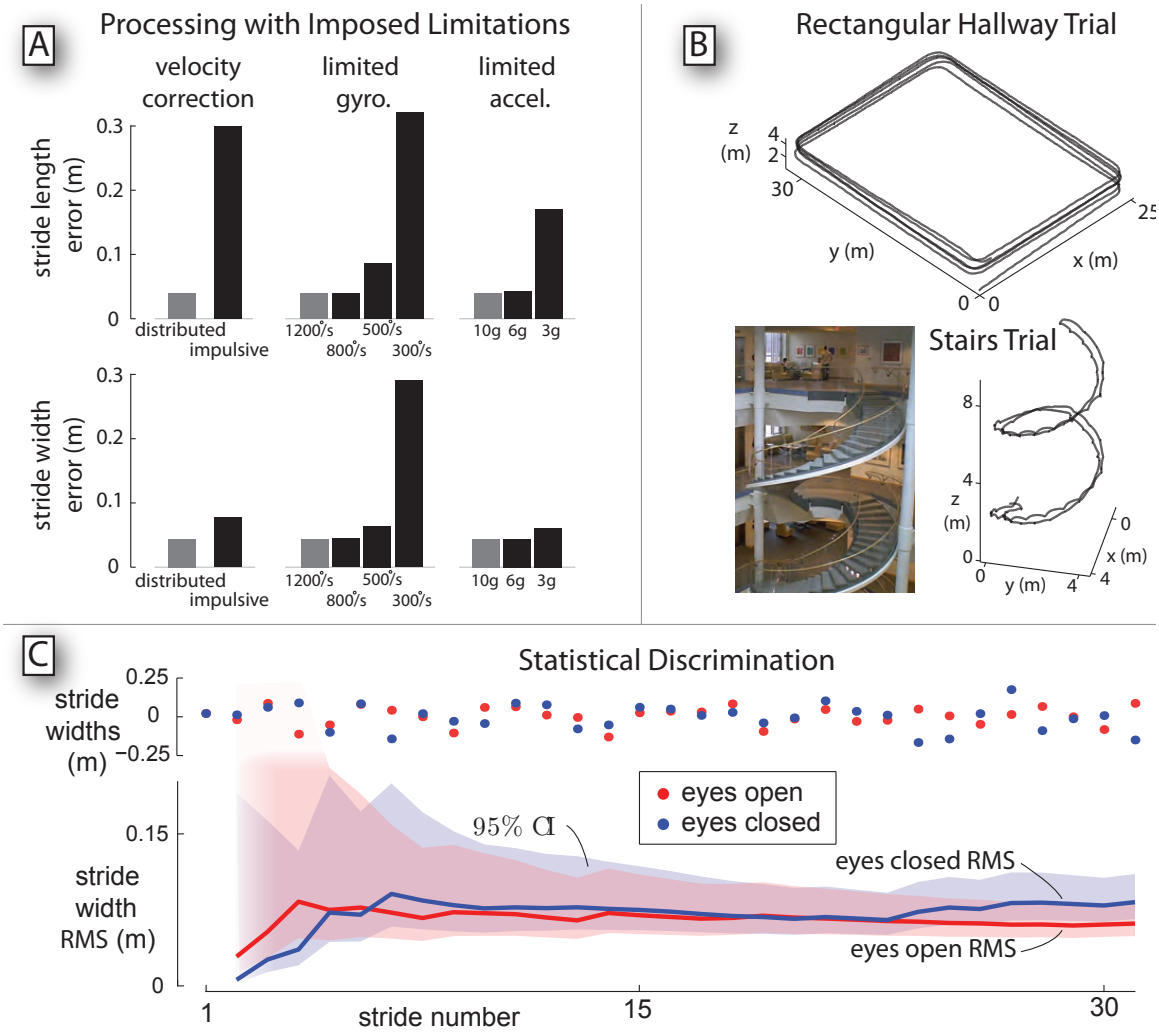

Figure 2.5: Limitations and extensions of inertial measurement of walking. **A:** IMU estimation errors with imposed limitations. Stride length (top) and width (bottom) errors are shown (relative to motion capture), using the proposed algorithm with a distributed versus impulsive zero velocity correction. Also compared are calculations made with artificially limited ranges for gyroscopes (between $1200\frac{deg}{s}$ and $300\frac{deg}{s}$) and accelerometers (between $10g$ and $3g$). Errors are summarized as standard deviation of difference between IMU and motion capture estimate. **B:** Demonstration of IMU processing applied to walking in non-laboratory environments. (Top:) Walking around a rectangular hallway circuit of approximately 110 meters, completed five times. (Bottom:) Walking up and down a set of spiral staircases (illustrated by photograph). Representative data from one subject show relatively low drift in absolute positions. **C:** Estimation of stride width variability as a function of number of strides. As individual stride widths are measured (top) from a representative subject, the estimate of stride width variability (bottom) improves in confidence (shaded areas for 95% confidence intervals).

variabilities.

Funding

This project was supported by Award Number R44AG030815 from the National Institute On Aging. The content is the responsibility of the authors and does not necessarily represent the views of the National Institute On Aging or the National Institutes of Health.

Disclosure

Mr. Rebula is affiliated with Intelligent Prosthetic Systems, LLC, which develops technology related to this research.

CHAPTER 3

The Stabilizing Properties of Foot Yaw in Human Walking

Humans maintain lateral balance during walking in a variety of ways, including lateral foot placement and ankle torque. A less recognized balance method is steering. We propose the use of foot heading for lateral balance, based on an analogy with methods of balancing a bicycle. If laterally perturbed, a bicycle will lean sideways about the forward (roll) axis, and steering the front wheel into the lean will allow the center of pressure to capture the center of mass laterally, avoiding a fall. We developed a dynamic walking model, where the passive dynamics of pendulum-like legs produce much of the walking motion, and we test the efficacy of foot heading to laterally stabilize this model. There are potential advantages to steering for stabilization in walking, such as the possibility to transform the direction of travel such that stable fore-aft dynamics can help dissipate the lateral perturbation. It is unknown whether humans actually employ steering for balance. We perform a human subject experiment of natural overground walking to test if steering is used alongside lateral foot placement to stabilize walking, in both Young and Elderly subjects. We find that stride width is correlated with foot heading step-to-step (total least squares fit slope of 0.38 radians per meter, intersubject t-test, $p < 0.05$). These results suggest that humans use lateral foot placement along with steering to laterally stabilize normal walking.

3.1 Introduction

Humans maintain their lateral balance during walking in a variety of ways. Two of the best recognized ways involve altering the center of pressure (COP) location underfoot, either with discrete adjustments to footfall location [8] or continuous application of torque about the stance ankle [41]. Less recognized is the possibility of steering the body about the vertical (yaw) axis for balance. This is illustrated by a bicycle, which can be stabilized by steering the wheel in the direction of leaning [63, 95]. In the case of human walking, it might also be possible to gain stability through a similar type of coupling, except by actively steering the foot's heading during swing. The central nervous system (CNS) might be expected to use whatever balance strategies are easy and available. But it is unknown whether active steering is comparable in effectiveness to the other balance strategies, and whether humans actually use it. We therefore seek to determine the potential effectiveness and employment of steering to maintain balance during human walking.

The role of steering for balance may be explained intuitively (Figure 3.1). For both bicycle and human in steady motion, the COP must, on average, remain under the center of mass (COM). A lateral perturbation to the bicycle will cause the COM to lean sideways about the forward (roll) axis, and steering into the lean will allow the COP to capture the COM. Not only can such steering stabilize against falling, but it can even be achieved passively with appropriate combinations of bicycle geometry and speed [63]. Interestingly, the bicycle can even gain some speed because it incorporates perturbations energy into the (newly-defined) forward motion. Walking is quite different from bicycle motion, because the successive footsteps create two alternating centers of pressure. But there may nonetheless be opportunity to steer for balance, in addition to the foot placement and ankle torque strategies [49]. This is demonstrated by a dynamic walking robot that stabilizes itself automatically with an ankle joint that kinematically couples steering with leaning [95]. In the case of the human, the ankle joint is not coupled kinematically, but the CNS might nonetheless choose to internally or externally rotate the leg as a function of roll-axis lean to maintain stability.

There are potential advantages to steering for stabilization. One is that steering allows soft and compliant control, where the perturbation can temporarily redefine the direction of travel. In contrast, foot placement control, and especially COP control, react more actively to a perturbation and attempt to restore motion to the original, nominal trajectory. That response could potentially be costly to perform, because the swing leg needs to be actively accelerated and because steps both narrower and wider than the nominal require more energy [26, 67]. Of course, in the case of steering, a perturbed direction of travel also requires

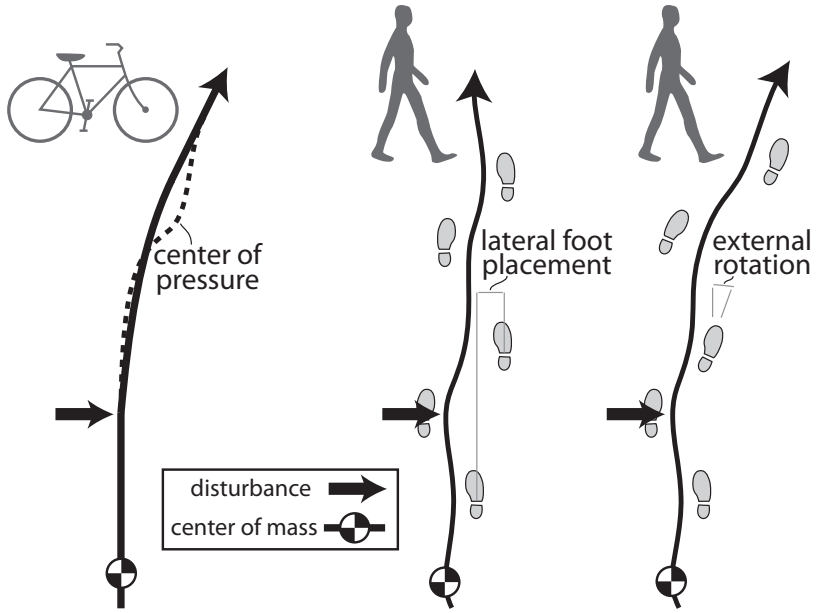

Figure 3.1: Conceptual model of lateral stabilizing with stride width and heading. A bicycle perturbed to the right can recover by steering the wheel to the right. A human perturbed to the right can recover by stepping out and/or altering the foot heading to the right. We propose that walking humans use both to maintain lateral stability.

a correction, but that can potentially be performed gradually and over longer time scales than immediate fall prevention. Thus, steering could be considered a means to extend the duration of response to a perturbation across multiple steps. It is also possible that steering could be combined with foot placement control, and allow for smaller adjustments in combination than either strategy alone.

It is unknown whether humans actually employ steering for balance. Such control would presumably require the CNS to sense motion of the body in three-dimensional space, determine deviations from the nominal gait, and apply corrections to the body heading, for example by externally or internally rotating the leg. It also remains to be determined whether the bicycle analogy, described qualitatively above, is indeed quantitatively feasible. In the present study, we therefore use a simple model of bipedal walking to demonstrate the feasibility of steering on balance. If humans steer for balance as demonstrated by the model, we would expect their footfalls to show correlations between foot heading (angle about the vertical) and lateral placement. We therefore examine the spontaneous deviations that occur during overground walking, and test whether they exhibit trends that agree with coupled steering and foot placement.

3.2 Methods

We will test the role of foot heading in stabilizing walking using a simple mechanical model of locomotion, and we will look for signs of foot heading stabilization in experimental human walking. We extended a simple model of 3d walking [49] by adding a mechanism to rotate the stance ankle in the vertical (yaw) direction. We considered lateral foot placement and external rotation as independent inputs to this linear system. We then generated stabilizing linear controllers based on these inputs to stabilize the walker laterally. By analogy with bicycle stabilization, we expected that foot heading and lateral foot placement should be positively correlated. That is, when perturbed to the right, we expected a stabilizing controller to command stepping more to the right, or pointing the stance foot to the right. We also analyze experimental human walking to estimate the use of foot heading. We observe the statistical relationship between lateral foot placement and foot heading, and we expect that humans use foot placement and heading in combination to laterally stabilize. We expect no such significant relationship between foot heading and fore-aft foot placement.

3.2.1 Model

We developed a dynamical walking model, where the passive dynamics of pendulum-like legs produce much of the walking motion (Figure 3.2, A). The model is similar to a previous one [49] with only two legs connected by a pelvis, that showed that passive dynamics can help stabilize forward motion, but not the lateral motion, which required active control such as through lateral foot placement. Following [49], we characterized stability of the model by linearizing the one-step return map, and analyzing the stability of this discrete linear system. We generated linear controllers to stabilize the system, where the signs of the control gains specify the appropriate stabilizing directions in response to a disturbance.

In order to characterize the effect of foot heading on the stability of walking, we developed a simple three dimensional model of walking, following [49]. Each foot was modeled as a portion of a cylinder that can roll forward upon the ground. Each leg attaches to a foot through a freely rotating hinge joint at the ankle that allows the leg to fall to the side about the roll axis. The legs are connected at the hips with a hinge joint that allows the legs to swing freely about the pitch axis, passing through the pelvis. There are also two additional degrees of freedom without passive dynamics. The first allows each leg to twist about its yaw axis with respect to the foot, to provide a means of steering. This was applied as a single angular deviation affecting both legs symmetrically. The second allows each leg to ab-/adduct relative to the pelvis, to allow for step width or foot placement adjustment. This was also applied to both legs as a single symmetric deviation. The walker is powered only by

gravity, walking down a gently declined ramp. Nonzero length, mass, and inertia properties of each the segments were chosen based on average human data [94] (Table 3.1). The unconstrained state vector is $x = \left[\text{roll}, \text{swingPitch}, \text{stancePitch}, \dot{\text{roll}}, \dot{\text{swingPitch}}, \dot{\text{stancePitch}}\right]$

We characterized stability of the model by assuming a nominal walking cycle and analyzing the stability of the disturbance response over a step. Based on a similar model of walking, we expect passive stability in the fore-aft direction and instability in the lateral direction [49]. We first found a passive limit cycle of walking with a step width dynamically comparable to human walking using a shooting method. We linearized the system about the fixed point at heelstrike, yielding a perturbation response matrix of partial derivatives, A. We also linearized the system with respect to the two inputs, leg splay angle and foot heading, to yield B_{splay} and B_{heading}, respectively. The stability of the resulting discrete linear system

$$\Delta x_{k+1} = A\Delta x_k \tag{3.1}$$

represents the stability of the full nonlinear walking system if it is assumed that any perturbations are sufficiently small. We therefore characterized the walker's stability using the poles of the linearized one-step return map. As in [49], we found a single unstable mode, corresponding to lateral toppling. To test the effect of each input on stability, we generated stabilizing linear controllers based on splay angle and foot heading independently, by considering the controlled system

$$\Delta x_{k+1} = A\Delta x_k + Bu_k \tag{3.2}$$

where $u = \Delta\text{legSplay}$, or $u = \Delta\text{externalRotation}$. Each input results in a corresponding B matrix, and pole placement is used to stabilize the unstable lateral falling mode. To generate a stable controller, we moved the unstable pole to a stable pole using minimal control effort, which corresponds to reflecting the pole about the unit circle. The signs of the resulting control gains determine the appropriate direction of lateral foot placement and the direction of the foot heading given a lateral perturbation.

The walking model suggests that active control of both lateral foot placement and foot heading can stabilize the lateral motion of 3d walking. The pole locations of the linearized one-step return map roughly approximated previous values for similar models [49]. An analysis of the open loop poles (Figure 3.2, B) show that there is one unstable pole (unstable poles lie outside the unit circle). The mode associated with this pole roughly corresponds to falling laterally about the roll degree of freedom at the stance ankle. As expected, if the walker undergoes a perturbation to the right (positive roll angle perturbation), the step width controller commands a step further to the right than normal, and the foot heading

Parameter	gravity	L	C	R	P	MPelvis	MLeg	ILeg	Kp
Value	1	1	0.645	0.3	0.3	0.68	0.16	0.017	0.1

Table 3.1: Walking model parameters. All parameters are dimensionless, normalized with respect to gravity, total mass, and leg length.

controller commands a rotation to point the foot further to the right than normal.

3.2.2 Experiment

We performed a human walking to experiment to estimate the use of foot heading to stabilize natural walking. As lateral foot placement is a known lateral stability mechanism, we observe the relationship between stride width and foot heading. If humans use both foot placement and heading to control lateral stability, we expect a positive correlation between these two measures, corresponding to the expected prediction for the simulation model. That is, when a foot is placed further to the right than normal, we expect the foot will also point further to the right than normal. Furthermore, we expect no such significant relationship between foot heading and fore-aft foot placement, as fore-aft foot placement does not have a strong effect on lateral stability. We use inertial measurement units to capture many contiguous steps of human walking to facilitate statistical analysis.

We collected healthy human walking data using foot mounted inertial measurement units [72]. Subjects walked in a straight hallway (roughly 90 contiguous steps). Subjects were separated into Young (N = 8, mean $\pm$ standard deviation age: 22.5 $\pm$ 1.5 years, 4 female) and Elderly (N = 14, mean $\pm$ standard deviation age: 67.4 $\pm$ 6.8 years, 9 female) groups. Subject consented to participation pursuant to institutional review board procedures. To calculate stride width and foot heading, the inertial data are processed to estimate the position and orientation trajectories of the foot [72]. This method has been found to match motion capture to within a few percent when measuring stride variability, but unlike motion capture, captures walking bouts of arbitrary lengths and durations.

The estimated foot trajectories are used to calculate stride length, stride width, and foot heading. Foot trajectories are first separated into individual strides using stance periods estimated based on low inertial sensor activity. These stride trajectories are then transformed into a local stride frame by defining forward as a linear fit to the last 3 stance period foot positions [72], and defining the origin as the initial postion of the foot in the stride (Figure 3.3). Stride length is defined as forward displacement in the stride frame, and stride width is the lateral displacement in the stride frame. Foot heading is calculated by considering a vector fixed in the inertial measurement unit frame. A heading is read during each stance

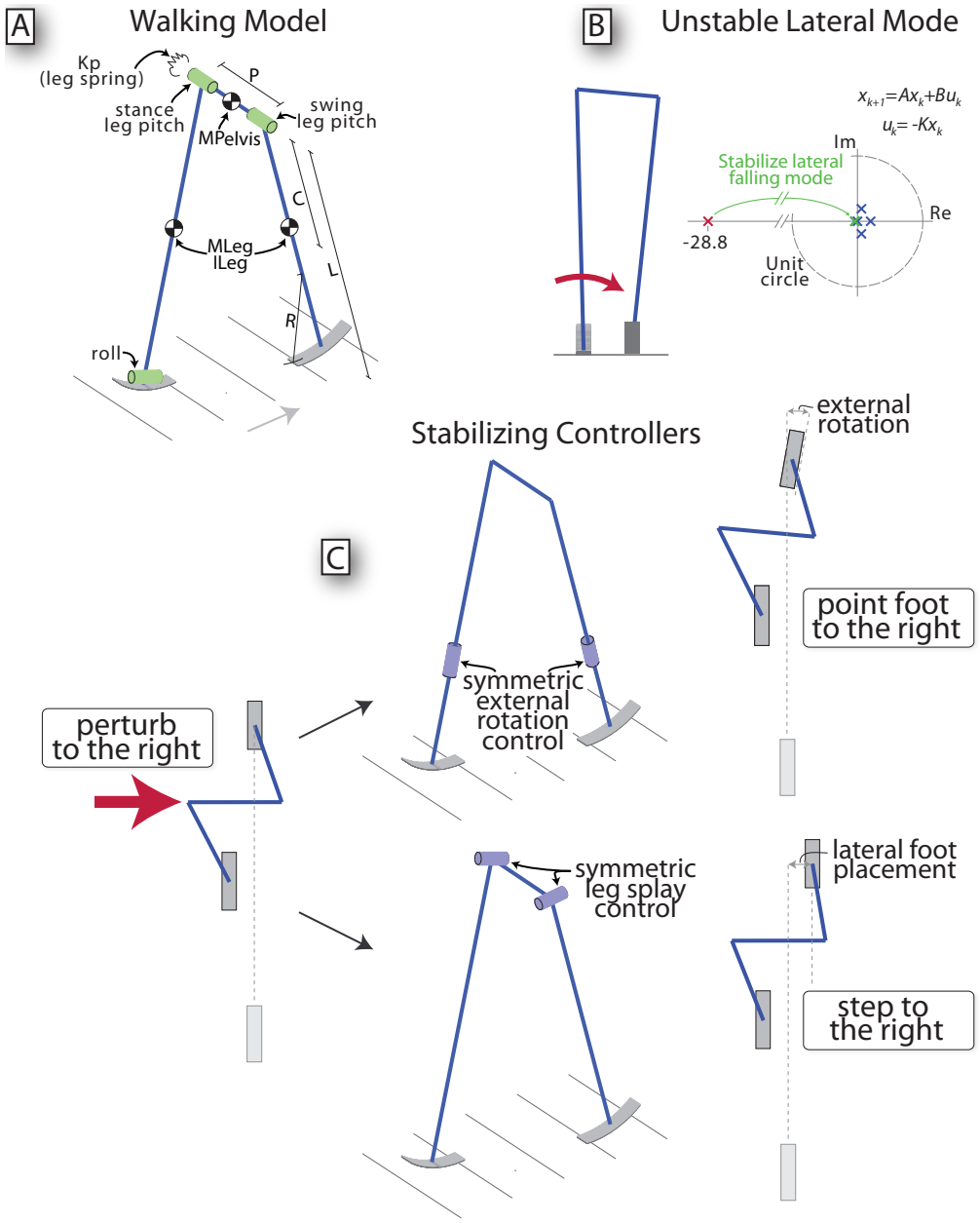

Figure 3.2: The walking model. (**A**) A limit cycle of walking is found with roughly anthropomorphic gait properties. (**B**) Linearizing the limit cycle one-step return dynamics about a fixed point at heelstrike yields a linear system $x_{k+1} = Ax_k + Bu$ (top). A B matrix is individually calculated for a lateral foot placement input and an external rotation input. The natural dynamics can be described by the open loop poles. One mode, corresponding to lateral toppling, is unstable (red, outside of the unit circle), and the rest are passively stable. (**C**) Two proposed linear controllers are tested, one using only lateral foot placement, and one using external rotation. Each controller is designed by pole placement, stabilizing the unstable lateral falling pole using minimal control effort (reflecting the pole about the unit circle). The control gain matrix for each input type indicates the appropriate control response given a roll perturbation to the right. We find that the model, when perturbed to the right, should either step out to the right, or point the foot more toward the right.

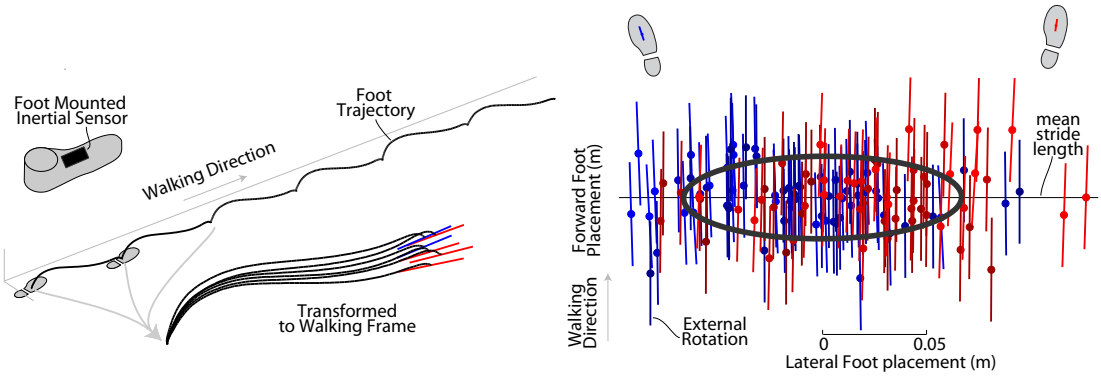

Figure 3.3: Step parameter calculation method. Inertial meausurement units are attached to subject's feet. The subject walks down a hallway, and the inertial data is processed to estimate the position and orientation of the foot. The foot trajectory is broken into individual strides, and transformed to a walking frame with the initial position at the origin. The variability of a walking bout for a single subject is estimated by observing the foot placement and orientation in the walking frame (right). The covariance ellipse (black) represents one standard deviation of variability. The lines corresponding to each footfall represent the external rotation of the foot for that stride, colored from blue (positive rotation, pointing to the left) to red (negative rotation, pointing to the right).

phase by calculating this vector's angle about vertical. The heading from three steps is used to estimate the subsequent step's local forward direction. The foot heading deviation for a given footfall is the heading minus the local forward direction.

We expect a positive correlation between stride width and foot heading. For each subject, the covariance matrix for stride length, width, and heading is calculated based on all strides for both feet. To test for a relationship between stride width and heading, we perform a t-test on the slope of the total least squares linear fit of heading versus stride width for all subjects. We expect the heading/width slope to be positive, based on our model expectations by analogy with bicycle balance. That is, we expect that when a foot is placed further to the right than normal, the foot will also point further to the right than normal.

We do not expect a significant relationship between stride length and foot heading. Similar to the heading versus stride width test, we perform a t-test on the heading versus stride length slope from all subjects. We do not expect a strong relationship between stride length and foot heading because we are estimating stride measures, as opposed to step measures. Stride length, for example, is measured as a displacement between the position of a foot during stance phase and the position of the same foot in the subsequent stance phase. In contrast, step length is measured as a displacement between the left and right foot. Correlations have been found between step length and step width [8], but we believe these length-width correlations will be eliminated when considering stride measures. Stride

	All subjects	Young	Elderly
Speed (m/s)	1.39 ± 0.165	1.42 ± 0.139	1.37 ± 0.186
Speed variability (m/s)	0.0483 ± 0.0221	0.0458 ± 0.0137	0.0502 ± 0.0273
Stride Length (m)	1.43 ± 0.152	1.48 ± 0.078	1.38 ± 0.182
Number of Strides	125 ± 20	120 ± 18.3	130 ± 20.9

Table 3.2: Gait parameters by subject group. Parameters are reported as mean $\pm$ standard deviation.

length-width relationships could be predicted by composing the left foot's step length-width relationship with that of the right foot. Since the length-width relationships are left-right symmetric, we expect this composition will result in no apparent relationship between stride length and width.

3.3 Results

Human experiments show a positive slope of the linear fit between stride width and foot heading. A line was fit (in a total least squares sense) to the foot rotation versus stride lateral foot placement data for all strides from all subjects. Similar fits were obtained for forward versus lateral foot placement, and foot rotation versus forward foot placement. The average slope for the rotation versus lateral placement fit are 0.38 (significantly different from zero), while all other slopes are not significantly different from zero. That is, when stepping 1cm further to the right than normal, the foot is also pointed 0.2 degrees further to the right more than normal.

Covariance ellipses calculated from all strides and subjects in each group were calculated for forward-lateral placement, rotation-lateral, and rotation-forward (Figure 3.4). For both Young and Elderly groups, there is less covariance in the forward-lateral and forward-rotation relationships than in the rotation-lateral relationship (Figure 3.4). No statistically significant relationship was found between fore-aft foot placement and foot rotation, or fore-aft foot placement and lateral foot placement (Figure 3.5). To identify any differences between the Young and Elderly groups, we performed a two-sample T-test on the individual slopes representing the rotation-lateral foot placement relationship, and found no statistical difference ($p = 0.75$). Gait parameters, such as stride length, speed, and speed variability, were similar between subject groups (Table 3.2).

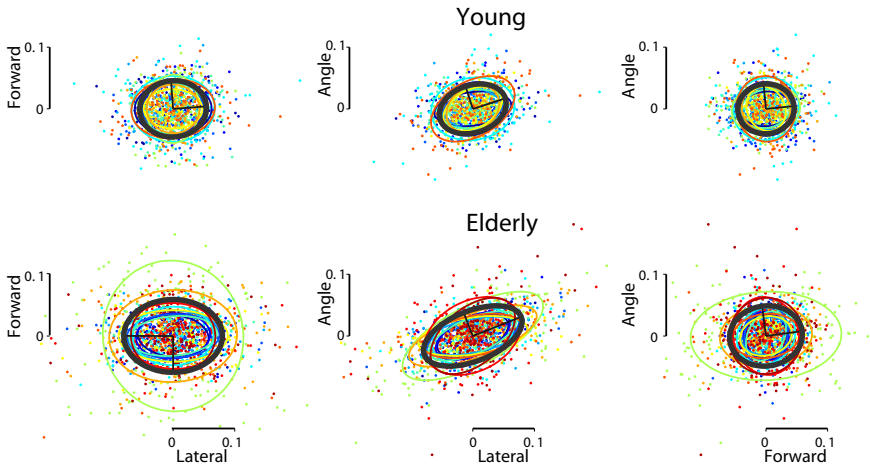

Figure 3.4: Covariances of step parameters. Step parameters for all steps are shown for Young (top) and Elderly (bottom) subjects. Note the priniciple axes of the overall covariance ellipse (black) for both Young and Elderly subjects have positive slopes, whereas the covariance ellipses for the other relationships exhibit no significant slopes.

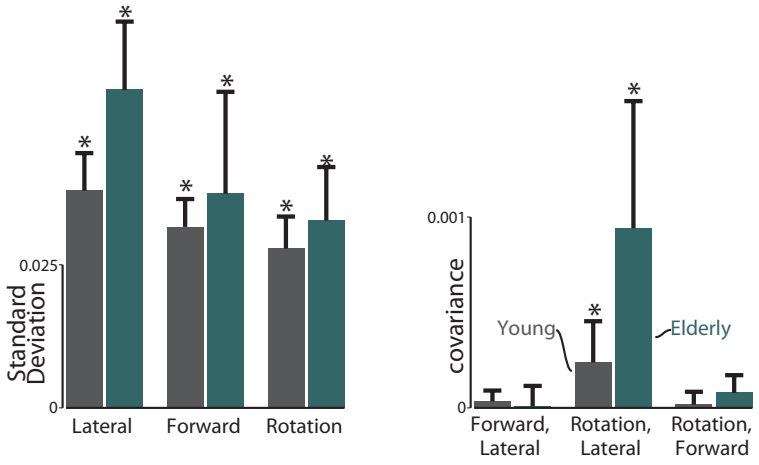

Figure 3.5: Summary of variability results. Elderly subjects show greater variability in lateral foot polacement than Young (left). Young and Elderly subjects showed similar variability in foreward foot placement, and foot rotation. All error bars represent inter-subject standard deviations of the given metric, asterisks denote significant difference from zero at a 1% confidence level. Significant covariance was observed between external foot rotation and lateral foot placement (right) for both Young and Elderly subjects.

3.4 Conclusions and Questions

We had saught evidence for the effectiveness and use of foot heading to stabilize human walking laterally. Our results suggest that foot heading is used as a lateral stabilization mechanism. Based on our walking model, foot heading can stabilize the lateral mode of walking in the same manner as steering a bicycle. In humans, we observed a statistical correlation between lateral foot placement and foot rotation, but not between foreward foot placement and rotation, indicating the possible use of foot rotation to stabilize human walking laterally. In the remainder of this section we consider the limitations and possible implications of this study.

As expected, the walking model can be stabilized by using the rolling foot to turn into falls like a bicycle. This agrees with previous research on directly coupling heading with roll [95]. Furthermore, the control gains calculated for stabilizing using leg splay angle and foot heading angle are of similar magnitudes:

$$K_{\text{lateral}} = [-2.076, -0.233, -0.013, -2.207, -0.291, -0.001] \text{ , and}$$
$$K_{\text{rotation}} = [-4.594, -0.516, -0.028, -4.883, -0.643, -0.002,].$$

This suggests that any system, human or machine, which minimizes overall control effort (acting, for example, as a linear quadratic regulator) would emply both mechanisms significantly during walking to avoid falling laterally. In human walking, we observed a correlation between stride width and foot heading, which is consistent with the hypothesis that humans use both lateral foot placement and external rotation to control lateral balance. Furthermore, no such correlation was found between stride length and foot heading, which was also expected due to stride length being more associated with fore-aft stability, and being only weakly related to lateral stability [49].

One limitation of the present study is the relative simplicity of the walking model, potentially limiting its predicitive power. The current model has relatively few parameters and assumptions. We believe the qualitative conclusions drawn from the modelling study to be relatively robust to these parameters and assumptions. Therefore we believe the finding that foot heading can stabilize this model to be a general property of 3d bipedal walking. As such, we do not consider the numerical results, for example the relative control gains of using stride width versus foot heading, to have a particular meaning in human walking, we only expect the signs of these gains to be relevant. No attempt is made, for example, to compare the amount of muscular effort required to rotate the body about the stance foot ankle versus the amount of muscular effort required to splay the legs. Furthermore, we only consider one mechanism by which the foot heading can be altered step-to-step. The foot can also change heading just during swing, without effecting the body dynamics.

While the foot may undergo this type of rotation in human walking, we have shown here the stabilizing effect of altering heading using a relative rotation between the stance ankle and pelvis. Further modeling and experimentation could illustrate tradeoffs between the various lateral stability mechanisms in human walking.

Another limitation in this study is the observational nature of the human walking analysis. Experimentation of additional conditions that isolate the stabilizing effect of foot heading would further illustrate its role in human walking. One possible alternative explanation of the correlation between stride width and foot heading is a simple kinematic coupling. For example, consider a subject with a very long foot, with the inertial sensor placed at the end of the toe. We would then expect foot heading angle change from step-to-step to result in a stride width change proportional to the distance from the center of rotation foot to the sensor. However, if the center of rotation of the foot is taken to be the ankle joint, the sensor was placed close to the ankle (e.g., at a distance of 0.05m), the expected coupling between angle and stride width would be an order of magnitude lower than observed (a coupling 0.05 rad/m as opposed to the observed 0.38 rad/m). Therefore, we believe that the coupling between stride width and foot heading is indicative of lateral stability control in normal walking, and this may be further revealed through overground perturbation experimentation.

While we have focused on natural overground walking, it is possible that the use of foot heading as a balance mechanism is dependent on the context of the locomotion activity. For example, humans walking on treadmills may be more constrained in their choice of foot heading than natural overground walking. Therefore, treadmill walking may rely on foot heading for stability differently than in natural walking. Treadmill walking involves a cumulative constraint on stride width on the order of the treadmill width; total lateral deviation must generally remain well below a meter. This has been found to alter lateral foot placement variability on treadmills [73]. Treadmill walking involves a similar constraint on cumulative foot heading (on the order of the inverse tangent of the treadmill width divided by length). Therefore, we expect that humans might use foot heading differently from natural walking when walking on a treadmill. Recent advances in gait estimation using inertial sensors has allowed capture of many overground steps, facilitating statististical analysis in the present study [12, 58, 72]. Inertial sensors are unobtrusive and can capture foot placement in long bouts of natural walking outside of lab environments, so they are ideal for measuring subtle statistical relationships in spontaneous walking.

While we here have shown the connection between steering and lateral stability for healthy subjects, considering foot heading could potentially improve treatment for patients with movement disorders. For example, a pathology might limit the patient's ability to

control foot heading, and therefore limit its use as a stabilizing mechanism. Or a pathology might compromise a patient's estimation of the body's roll angle, which the subject might attempt to correct with a foot heading, destabilizing the gait laterally. The inability to finely control foot heading might indicate a fall risk. In addition, it may be interesting to observe how subjects with, for example, transtibial amputation use heading to maintain balance in the absence of the ankle ab/adduction joint, although medial/lateral rotation of the hip is intact. The role of foot heading in lateral balance may also have implications for the control of robots, as it suggests that balance control should not be considered independently of a global heading control. Since heading and stability are coupled, a controller that incorporates foot heading into stability control could outperform a controller that neglects this mechanism.

CHAPTER 4

The Value of Smoothness in Bipedal Locomotion: A Simple Optimization Study

Humans prefer to walk and run with energetically economical gait patterns. Optimization models show that mechanical work, one of the main contributors to metabolic energy expenditure, is minimized when the legs act like stiff pendulums for walking, and stiff pogo sticks for running [83]. Stiff models explain some abstract aspects of ground reaction forces produced by humans, such as a double-peaked profile for walking and a single peak for running. But they also predicts force profiles that are unrealistically stiff and impulsive compared to humans, who produce much smoother profiles with longer ground contact durations. Although these differences might be explained by physical features such as elastic tendons, it is also possible that humans have additional metabolic costs beyond work. Here we consider metabolic costs for activating muscle that can theoretically explain the smoother profiles of human forces. Optimization for a combined energetic cost for work and rapidly fluctuating force produces the characteristic double-peaked force profile of human walking (coefficient of determination between model fit and human data is $R^2 = 0.96$) and single-peaked profile of running ($R^2 = 0.92$), more so than work minimization alone ($R^2 = -0.79$ and -12.0, respectively). Costs based on simple production of force resulted in less humanlike forces than costs based on force fluctuation. The proposed model presupposes no pattern for the leg forces except to satisfy constraints for periodic gait at a nominal movement speed and step length. It nevertheless discovers smoothed pendulum-like walking gait at lower speeds, and smoothed pogo-stick running at higher speeds. Although physical elasticity appears to be important in human locomotion, humanlike locomotion can be predicted without physical elasticity. It might be economical for humans to walk or run in a seemingly elastic manner, even if they did not have elastic tendons.

4.1 Introduction

Human locomotion is governed in part by metabolic energy economy. For a given speed, aspects of an individual's preferred gait are normally associated with a minimum of energetic cost [52]. Alterations to variables such as the preferred stride length [27], stride width [26], and vertical displacement of the body [35], typically lead to increased energy expenditure. However, some gait features are quite stereotypical but not obviously determined by economy, notably the ground reaction forces. Their profiles might somehow be linked to economy, because forces are the product of muscles, which perform mechanical work and thus expend energy. But it is not clear how energy economy might dictate the forces characteristic of human gaits. Here we investigate possible contributions to metabolic energy that might indeed govern the forces exerted during locomotion.

One significant energetic cost in locomotion is for the production of mechanical work. In human muscle, positive work is performed at a metabolic energy efficiency of about 25%, and negative work at about -120%, so that both cost positive energy (e.g., [57]). During walking, work is needed to redirect the body center of mass (COM) between pendulum-like steps [53]. A simple two dimensional walking model [50] shows that kinetic energy is lost when a pendulum-like swing leg collides with the ground. Energy may be restored most economically by applying an ideal impulsive (instantaneously short) push-off force along the trailing leg just prior to the leading leg's collision, because it reduces the associated energy loss. However, humans also appear to perform push-off work, with a proportional energetic cost [26, 53]. An alternative model relaxes the inverted pendulum assumption, and allows for arbitrary leg forces, only constraining the model to produce a walking gait in two dimensions [83]. Even given arbitrary possible gaits, optimization for minimum mechanical work predicts walking with rigid, pendulum-like leg behavior, with impulsive push-off and collision (Figure 4.1). The same optimization applied to running also favors impulsive forces separated by aerial phases [83]. These optimizations suggest that one strategy for reducing mechanical work would be to attempt to walk and run with straight legs, producing instantaneous push-off and collision forces.

In actuality, human legs only partially behave as pendulums. The ground reaction forces stereotypically exhibit two peaks that abstractly resemble the impulses predicted to minimize work, except with considerable smoothing (Figure 4.1). Ideal impulses are theoretically economical because they redirect the COM velocity with minimal work [53]. Yet humans do not produce perfectly instantaneous forces [93], and would therefore appear to perform more than the minimum possible displacement and work. We will investigate a criterion that penalizes aspects of the produced force which, in addition to mechanical

work, might better explain human locomotion than analysis of mechanical work alone.

An alternative to the rigid-legged model is to treat the legs as perfectly elastic springs that also move somewhat like pendulums. Models with axially compliant legs [33] yield ground reaction profiles more similar to human, for both walking and running. But these models have no dissipation and perform no work, and therefore have no energy cost for any stiffness, unlike humans [99]. Their legs do have some elastic properties owing to spring-like tendons [3], but the muscles must still perform considerable positive and negative work with non-zero metabolic energy cost [57]. This raises the question of why humans legs behave so much like springs [62], when they are not physically springs, and when less work would be required if they behaved more like rigid pendulums.

The discrepancy between models might be explained by another cost, not accounted for by mechanical work alone. A number of other costs have previously been proposed for the optimization of various motor tasks. One of the simplest is the time-integral of force (tension-time integral, [40]), associated with the metabolic energy cost of isometric force production. Another is the time-integral of muscle force or activation raised to the second (or higher) power, integrated over the time duration of the movement. Its physiological basis is less clear, but could be related to motor performance, as movement uncertainty increases with force magnitude (due to signal-dependent noise, [38]). Another interpretation is that the exponent describes a metabolic cost, because greater force entails recruitment of less efficient motor units within a muscle [43,88]. But even though the physiological explanation may be unclear, optimization studies often require a force-squared or similar term, without which the optimum may call for unrealistically high force application (or bang bang control, [82]). There are, of course, physical limitations on muscle force magnitude, and so it could also be argued that there should be an optimization cost for peak force. In addition, we will consider costs that penalize rapid fluctuations in force, calculated based on the derivative of the force profile. Previous experiments of periodic movements such as leg swinging [24] and bouncing up and down using ankles [23] have suggested a metabolic cost that may be based on the speed of force changing, independent of mechanical work. Although each of the above costs is plausible, it is unclear which (or whether) any of them could explain the force profiles observed in locomotion.

In the present study, we apply a general model of force-like costs to the optimization of bipedal walking and running. We used a very simple, computational model starting with a cost for mechanical work, similar to that of Srinivasan & Ruina [83]. To that objective was added another term that could be parametrically adjusted to penalize the integral of force, or force-squared, and other force-like variations. We also applied an adjustable weighting between work and the force-like cost. With a cost for work alone, the model favors

impulsive forces and rigid legs. With the force-like cost alone, it may favor very different force profiles that, in combination with work, may bear greater resemblance to human. The model is a simple two dimensional point mass mechanical model of walking, without considering muscle dynamics or many other complications associated with humans. From this study, we seek to determine whether some force-like hypotheses are unlikely to help explain human gaits. It is possible that a relatively simple addition to the model of Srinivasan & Ruina could better explain the ground reaction forces observed in actual walking and running, compared to the cost for mechanical work alone.

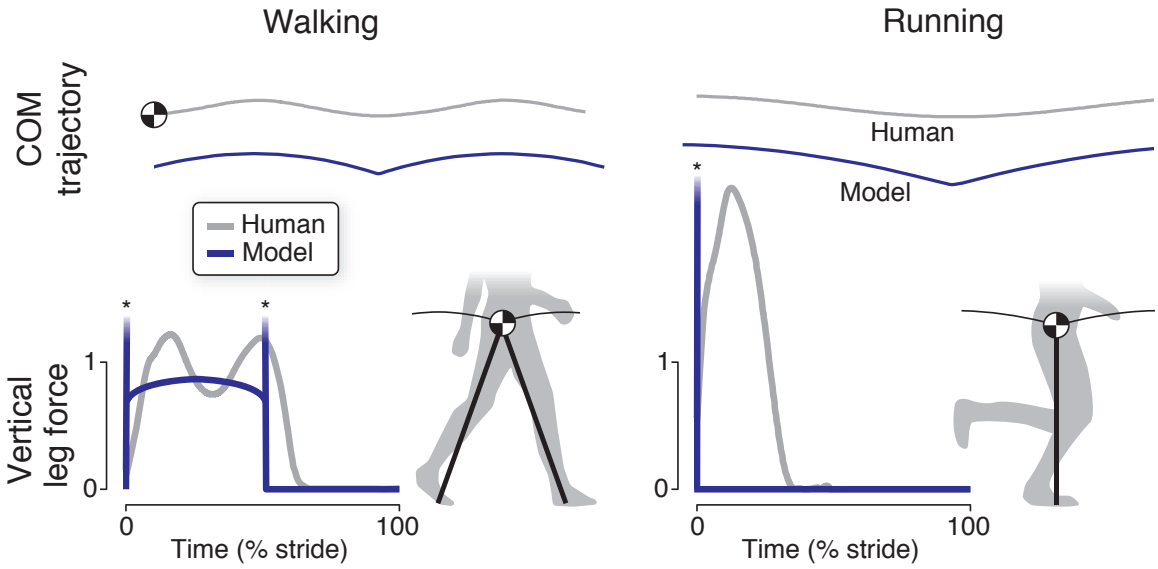

Figure 4.1: Comparison of work-minimizing model of locomotion with human walking and running gaits. Comparison of work-minimizing gait with human gaits, in terms of body center of mass (COM) trajectories and vertical ground reaction forces versus time. The model's COM trajectories feature a sharp, instantaneous redirection due to ideal impulsive vertical ground reaction forces (asterisks denote infinitly high peaks, shown truncated) in both walking and running. In contrast, human gait has much smoother COM trajectories and more rounded vertical leg forces with finite peaks.

4.2 Methods

We formulated a computational optimization problem to produce periodic, bipedal locomotion (Figure 4.2). The locomotion model is planar and consists of two massless legs that rotate freely about a pelvis, modeled as a point mass, roughly approximating the location of the human body's center of mass (additional details of the model and optimization problem are given in Appendix A). The legs can actively telescope and exert arbitrary axial forces

over time, as in the model of Srinivasan & Ruina [83]. The force are applied along the axis of each leg, in direction determined by each leg's ground contact point with respect to the pelvis. The optimization is intended to allow for a wide range of possible center of mass trajectories and a wide variety of gaits, such as walking and running. It includes a small number of constraints defined primarily to enforce steady, periodic gait with left-right symmetry. For comparison with experimental data from humans, we consider two nominal gaits: walking at a speed of 1.25 m/s and step length of 0.68 m, and running at 5.0 m/s and step length of 1.5 m (see Appendix A).

The optimization searches over trajectories of leg forces and body states to find a gait. A minimal representation of a gait comprises two leg force trajectories over one locomotion step (with duration T_{step}) , and a set of initial conditions for the periodic cycle (i.e. a fixed point of a limit cycle [84]). The body states are defined as the forward and vertical positions of the point mass pelvis (x and y, respectively) and their time-derivatives (velocities $\dot{x}$ and $\dot{y}$, respectively). Each leg force magnitude trajectory (f and $f^{'}$) is described by a piecewise linear function between N control points, describing the axial force between pelvis and foot. The force trajectories are for one step of locomotion, equivalent to half a symmetric stride (the time between successive heelstrikes of a single leg). When both feet are on the ground, they are separated by the given step length (L_{step}). When one foot is on the ground, the swing leg is instantaneously advanced forward by one step length, after which the two leg forces are swapped to produce the second step of a stride. All state variables and other quantities are nondimensionalized using pelvis mass M, a maximum allowable leg length L, and gravitational acceleration g as base units.

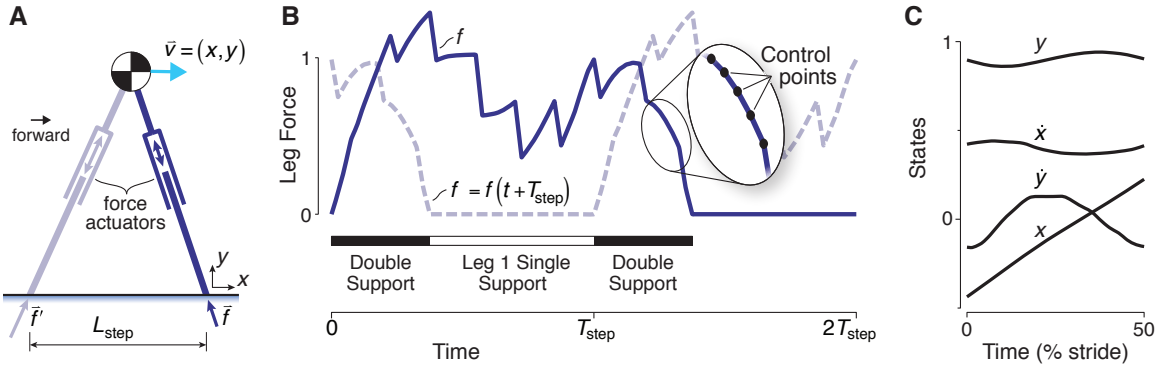

Figure 4.2: Optimization model for bipedal locomotion. (A) The model has a point mass body and massless, telescoping legs driven by axial force actuators. (B) Force magnitudes are represented as piecewise linear functions of time within a step (defined by control points, magnified in inset). (C) The state vector includes body positions and velocities ($x, y, \dot{x}, \dot{y}$; lower left), which result from the leg forces and equations of motion.

Several constraints are applied to ensure proper gaits. The states must obey the dif-

ferential equations of motion for the body with the leg forces as input. A maximum limit is also enforced on leg length, measured as the distance between pelvis and a foot on the ground. The leg's force trajectory is constrained to zero at the beginning and end of the stride to guarantee a minimum (and possibly very brief) duration for a swing phase. To enforce continuity, leg force at the end of a step is constrained to be equal to the other leg's force at the beginning of its step. To ensure steady locomotion at the nominal speed, the pelvis position and velocity at the end of each step are constrained to be equal to the initial pelvis state translated forward by the nominal step length, with a duration appropriate for the nominal speed. There are no features explicitly specifying walking or running gaits, which must therefore emerge from the optimization alone, as a function of the given movement speed and step length. Details of the constraints and dynamics are provided in Appendix A.

We define an independent weighting parameter to adjust the tradeoff between the proposed work and force costs. The overall objective function J is the weighted sum of a work cost J_w and a force cost J_f:

$$J = (1 - \alpha)J_w + \alpha J_f \tag{4.1}$$

where α is the relative weighting, ranging from 0 to 1. The value $\alpha = 0$ denotes minimization of work alone, and should yield impulsive walking or running [83]. In contrast, $\alpha = 1$ denotes minimization of the force cost alone. At intermediate α values, we expect to see the effect of combining the work and force costs.

We define the work cost as the integral of the rectified mechanical power of both legs over a step [83]:

$$J_w = \int_0^{T_{\text{step}}} |\vec{v} \cdot \vec{f}|_* + |\vec{v} \cdot \vec{f'}|_* \tag{4.2}$$

The absolute value places a positive cost on both positive and negative work. The two have different physiological costs [57], but any constant ratio between them is equivalent to an adjustment in the weighting α, thereby obviating the need for an additional parameter for that ratio. ($|\cdot|_*$ denotes a smoothed absolute value function, see Appendix A)

The other component of the total cost function is for force. To penalize leg forces, we define a cost of the form

$$J_f = ||f^{(n)}||_p := \sqrt[p]{\int_0^{T_{\text{step}}} |f^{(n)}|_*^p + \left|f'^{(n)}\right|_*^p dt}, \tag{4.3}$$

where $\vec{f}^{(n)}$ is the n^{th} derivative of force. We will investigate $n = [0, 1, 2]$, where $n = 0$ penalizes force amplitude, and greater values of n increase the penalty on higher-order rates

of change in force. We also investigate a range of p, where greater values penalize larger peaks in the force cost. This cost is intended to qualitatively model a physiological cost of force production or force fluctuation [23, 24, 55]. While various detailed models of low level muscle energetics have been proposed and used to analyze walking [55, 65, 88], we use simplified models of both locomotion dynamics and muscle energetics. These simplifications allow us to investigate various aspects of force cost and their potential effects on gait, independent of the particulars of a high dimensional model.

Optimized gaits are compared to human locomotion in three ways. First, we calculate a quantitative measure of the overall resemblance between profiles, using the correlation coefficient between ground reaction forces from model and human data (see Appendix A), for a range of values for the weighting α. Second, we examine the duty factor, defined as the time each leg contacts the ground, as a fraction of a stride, as well as peak force magnitudes, in comparison with human locomotion. Third, we examine the relationship between vertical leg force and vertical body displacement during stance, a relationship that is roughly linear in both walking and running gaits for a variety of animals [62]. We fit a line to calculate an effective vertical stiffness, which summarizes the overall oscillatory behavior as produced by active muscles and passive tendons. These various measures help to quantify the overall similarity between model and human.

4.3 Results

We found that the addition of a cost for force production reduced the maximum amplitude of the optimized walking forces. We examine sensitivity of the results to the two parameters of the force cost (Equation 4.3): the derivative order n and the norm exponent p. We sample values of n between 0 and 2 and various values of p (Figure 4.3). A force cost with $n = 0$ and $p = 1$ represents a penalty on the integral of the force amplitude. Including a cost for integrated force amplitude results in generally jagged forces, and changing the weighting α alters the optimal forces with no particular interpretable trend (Figure 4.3, "amplitude force costs", left). Adding a nonlinear power to the force amplitude ($p > 1$) penalizes production of larger magnitudes nonlinearly more than lower magnitudes. Optimizing with $p = \infty$ penalizes only the maximal force, resulting in an approximation of inverted pendulum walking, with brief square wave forces replacing the instantaneous collision and pushoff forces.

For $n = 1$ or 2, we interpret the force cost as a penalty on force fluctuation. When including a force fluctuation cost, the optimization yields broadly similar effects, but somewhat differing force profiles (Figure 4.3, "fluctuation force costs"). Variations of the force

fluctuation cost produce small differences in peak force, force profile, and double support period, and produce the most human-like forces for different intermediate values of α. But regardless of the particular parameter values, there is a general tendency to produce more rounded peak forces.

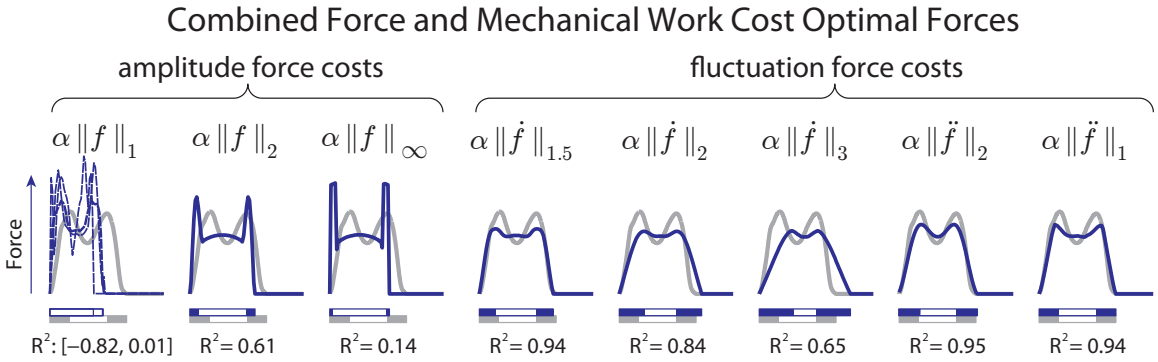

Figure 4.3: Vertical ground reaction forces for gaits optimized for force and work costs. Ground reaction force trajectories for various formulations of force cost J_f (Equation 4.3). Examples show the effect of varying the derivative order n and norm exponent p. Values for α were chosen to qualitatively match human forces where possible. The values for α in the cost function are (left to right), for amplitude force costs: $[4.5 \cdot 10^{-1}, 5.0 \cdot 10^{-1}, 5.5 \cdot 10^{-1}]$, $3.0 \cdot 10^{-2}$, and $1.0 \cdot 10^{-2}$, and for fluctuation force costs: $1.1 \cdot 10^{-4}$, $1.6 \cdot 10^{-3}$, $3.2 \cdot 10^{-2}$, $1.1 \cdot 10^{-2}$, $2.7 \cdot 10^{-3}$.

Optimizing only for force costs reveals two broad classes of solutions (Figure 4.4). Penalizing force amplitude alone yields force profiles with approximately instantaneous jumps in force (Figure 4.4, "amplitude force costs"). In particular, penalizing only the time-integral of force magnitude ($p = 1$) yields a single instantaneous force impulse. As p increases, the force-cost optimal profile resembles a square wave lasting the entire stride. This results in an instantaneously short swing period, with both feet on the ground producing force for essentially the entire gait cycle. There are jump discontinuities at the beginning and end of the stride. In contrast, optimizing for force fluctuation costs alone (Figure 4.4, "fluctuation costs") results in forces characterized by smoothly changing forces throughout the stride, with no jump discontinuities. This qualitative difference between amplitude and fluctuation costs illustrate the source of the qualitative difference between the combined force and work costs, as the jump discontinuities are seen in the amplitude force cost combined optimized results (Figure 4.3). As force fluctuation costs were generally better able to reproduce human walking forces (based on R^2 of model-data agreement) we will consider only force fluctuation costs in further analysis, in particular, $p = 2, n = 2$

Verifying the results from Srinivasan & Ruina [83], we found that minimization of work alone yields inverted pendulum walking (Figure 4.5, $\alpha = 0$). During most of single

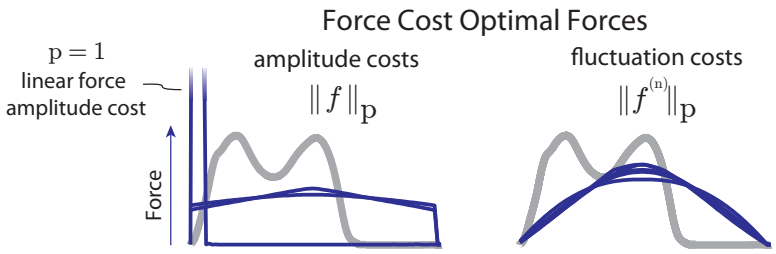

Figure 4.4: Vertical ground reaction forces for gaits optimized only for force costs. For amplitude costs ($n = 0$, left), the optimized forces resemble square waves or an instantaneous spike. For fluctuation costs ($n > 0$, right), forces smoothly rise from zero to a peak, then return to zero smoothly. All gaits (except a linear amplitude cost) exert leg forces for both legs throughout the stride except for instantaneous swing phases. In general, forces that optimize costs for force amplitude exhibit force discontinuities, while forces optimal for fluctuation costs have no discontinuities.

support, the leg is rigid, with no leg compression and therefore no work. Work is performed only at an impulsive collision at the beginning of a step, and a perfectly impulsive push-off at the end. The leg duty factor approaches 0.5, so that double support also approaches zero duration. Push-off from the trailing leg immediately precedes collision of the leading leg, similar to the ideal pendulum model [50].

We found that the addition of a cost for force fluctuations yields gaits bearing more resemblance to human (Figure 4.5). Starting with the work-minimizing gaits, an increase in the weighting α causes the leg forces to become less impulsive, transitioning to maximally smooth gaits when minimizing force fluctuation alone. An intermediate value of α produces leg forces qualitatively similar to human both for walking and running. Increasing α produces increased double support durations and decreased peak force magnitudes.

At the other extreme, minimization of force fluctuation alone yields an extremely smooth walking gait (Figure 4.5, $\alpha = 1$). The pelvis moves in a nearly level path, with both feet on the ground for nearly the entire step. The leg duty factor approaches unity, so that double support phases are separated only by infinitesimally brief single support phases to advance the swing leg. A relatively long stance phase allows the leg forces to grow and decay smoothly, resulting in relatively large leg displacements compared to the work-minimal gait.

With an intermediate weighting of force fluctuation and work costs, the walking optimization yields more human-like leg forces. These are characterized by a double peak in vertical ground reaction force, finite double and single support durations, and intermediate force magnitudes (Figure 4.5, $\alpha = 1.61 \cdot 10^{-3}$). The weighting α also causes a smooth transition between two extremes. Recall that a weighting on work alone tends toward a leg duty factor of 0.5 and perfectly impulsive forces, whereas minimization of force fluctuation

alone tends toward a duty factor of 1 and maximally smooth forces with low amplitude. As weighting α increases from zero, the two impulsive peaks in force decrease in amplitude and lengthen in duration, yielding two rounded profiles. Increasing α further, the two peaks combine into a single rounded peak. Increasing α also causes the work cost J_w to increase monotonically, just as the force fluctuation cost J_w decreases. Concurrently, the duty factor increases and the peak force magnitude decreases, both monotonically. The correlation with human ground reaction forces reaches a maximum of $R^2 = 0.96$ at an intermediate weight of $\alpha = 2.68 \cdot 10^{-4}$. This exceeds values of $R^2 = 0.79$ for work only, and $R^2 = 0.22$ for force fluctuation only.

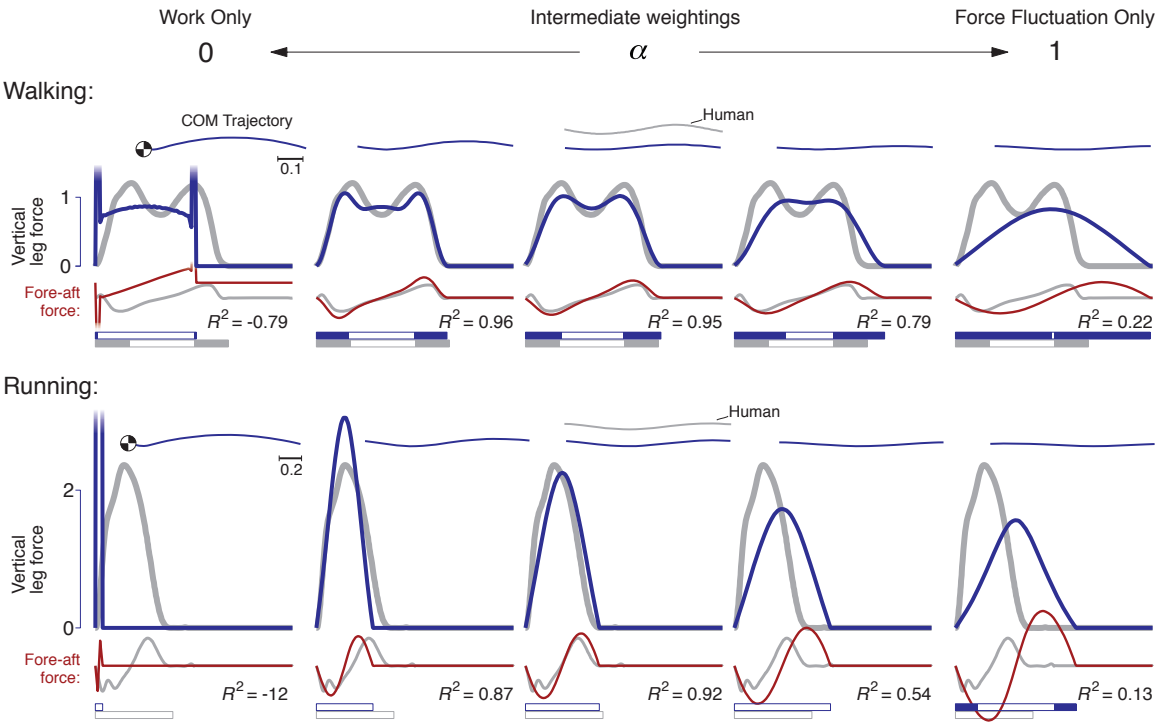

Figure 4.5: Optimized walking and running gaits. Optimized gaits as a function of weighting α. Shown are COM trajectories, vertical leg forces versus time, fore-aft leg forces versus time, and ground contact periods. Work-minimizing gaits (left side, $\alpha = 0$) approach impulsive walking (top) and running (bottom), while force fluctuation minimizing gaits (right side, $\alpha = 1$) have very smooth leg forces. Intermediate combinations of the two costs result in gaits with more human-like attributes, both in leg forces and in COM trajectories (shown in gray for human). Values for α for walking are (left to right): 0, $2.68 \cdot 10^{-4}$, $1.61 \cdot 10^{-3}$, $2.68 \cdot 10^{-3}$, and 1. Values for running are: 0, $2.15 \cdot 10^{-3}$, $8.05 \cdot 10^{-3}$, $5.37 \cdot 10^{-2}$, and 1.

Optimizing work and force fluctuation has similar effects for running. Minimization of work alone results in an impulsive grounded running gait with an infinitesimally brief ground contact, similar to that of Srinivasan & Ruina [83] (Figure 4.5). In contrast, mini-

mization of force fluctuation alone results in a very smooth gait with the pelvis following a nearly level path. As the weighting increases, the force profile remains single-peaked but becomes longer in duration and lower in amplitude (Figure 5.6). Near unity weighting, the aerial phase disappears, as the duty factor exceeds 0.5 and yields a brief double support period. An intermediate weight ($\alpha = 8.05 \cdot 10^{-3}$) results in a more human-like running gait with finite contact and flight phases. The correlation with human ground reaction forces reaches a maximum of $R^2 = 0.92$ with $\alpha = 8.05 \cdot 10^{-3}$. This exceeds values of $R^2 = -12.0$ for the optimization that minimizes work only ($\alpha = 0$), and $R^2 = 0.13$ for force fluctuations only ($\alpha = 1$).

We next examine the relationship between total vertical force and vertical center of mass displacement (Figure 4.7). Work-minimal walking and running tend toward infinitely stiff behavior, as indicated by the force-displacement slope, during pushoff and collision. With increasing α, the smoother walking exhibits lower vertical stiffness during double support, while an intermediate α value results in a peak single support stiffness. At an intermediate weighting, the model exhibits vertical stiffnesses that qualitatively agree well with stiffnesses fitted from human data. A similar correspondence holds for running. As α increases, the ground contact phase exhibits decreasing stiffness, again approximating that of human for an intermediate weighting.

The force-displacement profiles may also be examined more directly in terms of the axial leg forces (Figure 4.8). Here it is evident that all of the gaits tend toward a pseudo-elastic behavior [74], with force profiles that exhibit no work loops. Even though arbitrary forces may be obtained, the optimization generally favors profiles that could mostly be produced passively with springs, with one exception: Work-minimizing walking ($\alpha = 0$) requires that the spring store the negative work of collision, and not release it until push-off at the end of stance. Nevertheless, the general tendency is for axial forces to behave with lower pseudo-stiffness as α increases.

4.4 Discussion

We had sought to determine whether an objective penalizing leg forces could explain the rounded profiles for human ground reaction forces. A previous optimization model of locomotion performs a minimum of mechanical work [83] and predicts forces that resemble those of human in an abstract sense, except for unrealistically high amplitudes at push-off and collision, and unrealistically short double support duration. We found that an opposing extreme is to minimize force amplitude or fluctuations, which by itself yields walking with an unrealistically long double support phase and no appreciable single support. A combina-

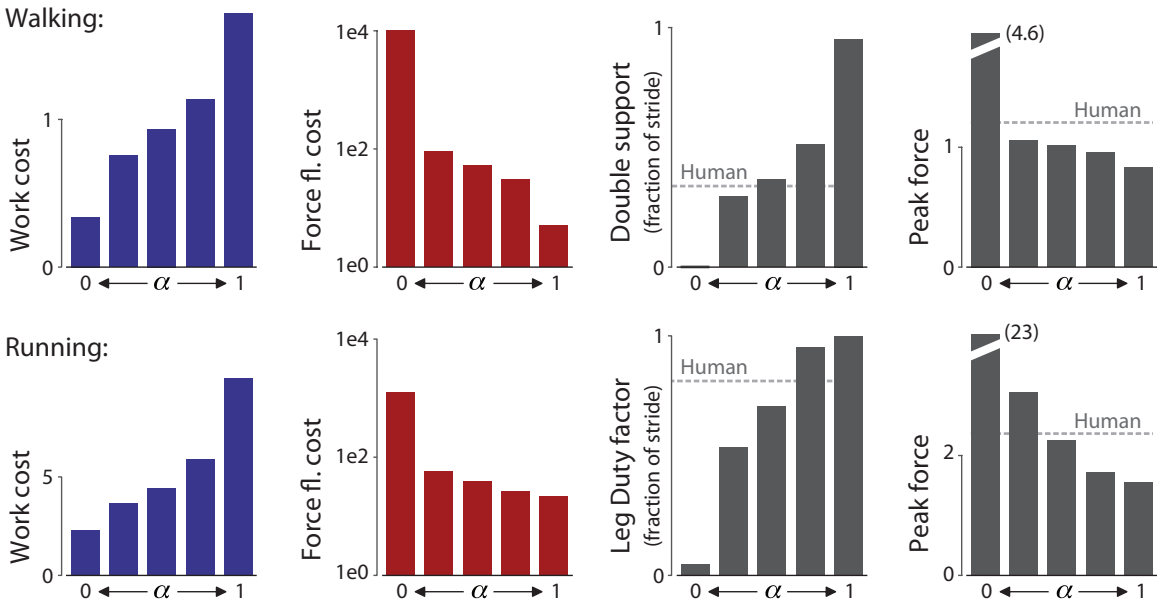

Figure 4.6: Summary measures of optimized gaits. Work cost, force fluctuation (fl.) cost, double support time (for walking) or leg duty factor (or ground contact time, for running) as fraction of stride, and peak vertical force. As the optimization cost function is changed from work only ($\alpha = 0$) to force fluctuation only ($\alpha = 1$), the work cost increases and force fluctuation cost decreases, both monotonically. Double support time and leg duty factor (ground contact time) increase, and peak force decreases. Values for human (shown as dotted lines) are between the extremes found at work-minimal and force fluctuation minimal gaits. All measures are dimensionless unless noted.

tion of mechanical work and force fluctuation costs can, however, produce double-peaked forces and support durations more characteristic of humans. We also found that costs based on force amplitude produced less humanlike walking. We found that relevant intermediate α values are very small, perhaps accounting for a unit conversion factor between N/s and mechanical watts. Below we examine possible implications of this model for human locomotion.

Optimizing walking using a combination of costs for mechanical work and force amplitude resulted in forces qualitatively different from human forces. In particular, a simple cost for force production ($n = 0, p = 1$) resulted in generally indeterminate force solutions with erratic force fluctuation (Figure 4.3). We believe this is due to the requirements of steady gait. Because the gait was constrained to a constant speed, the forces on the body must sum up to gravity over the course of the stride. Since a wide range of leg forces can satisfy the constraints of steady walking, it is perhaps not surprising that minimzing integral of the leg force magnitude has little effect on the optimal leg forces, since the vertical component is constrained to sum to body weight. Furthermore, optimizing for linear force

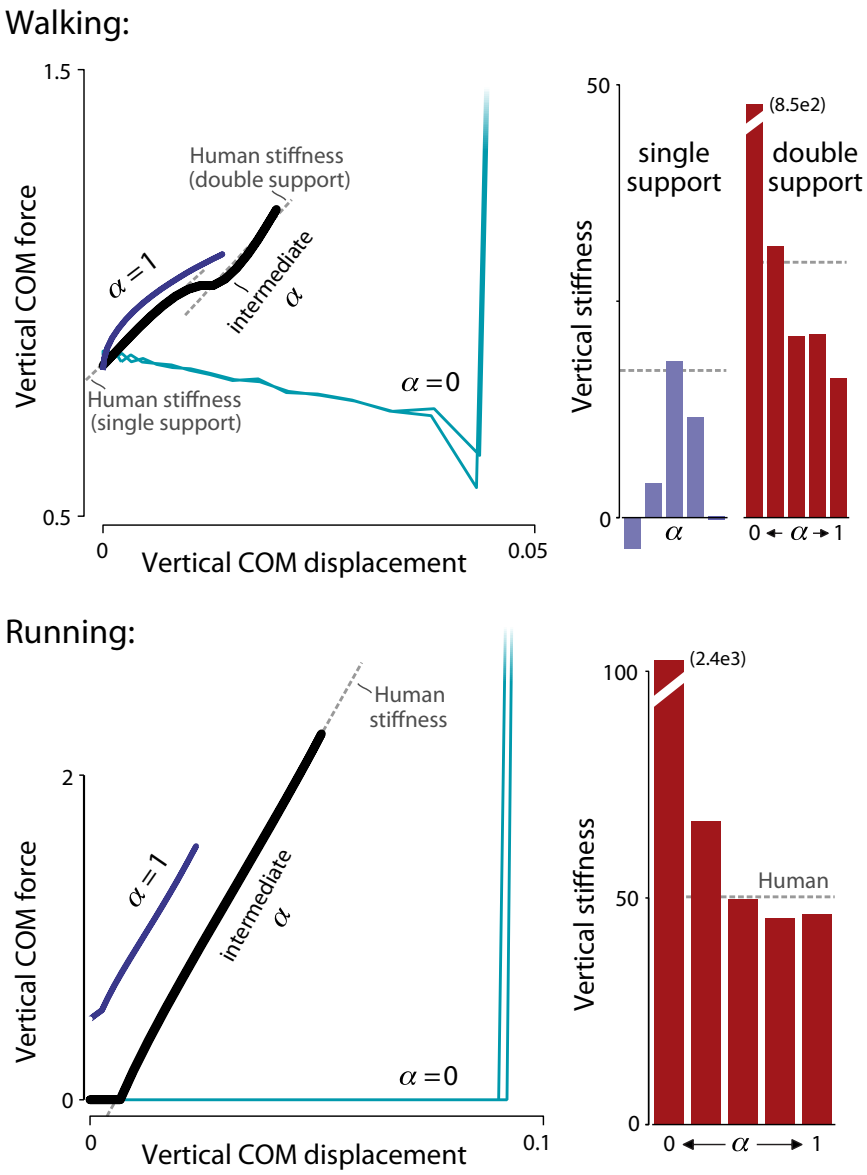

Figure 4.7: Vertical stiffness of optimized gaits. Force versus displacement (left) and vertical stiffness (right) for optimized gaits. The force versus displacement relationship shows multiple regions of effective stiffnesses, defined as the slope of the force-displacement curve. Optimization yields walking gaits with two stiffnesses, one relatively low during single support, and one relatively high during double support (with stiffnesses typical of human shown with dotted lines). Fitting line segments to these periods yields estimates of effective vertical stiffness (right) for the model, as a function of weighting coefficient α. Model results for intermediate α weights are similar to those of human.

amplitude alone resulted in a single spike of force, resembling the mechanical work optimal solution for running (Figure 4.4, "force amplitude cost"). Due to this similarity, adding a linear cost for force amplitude does not result in optimal force profiles qualitatively dif-

ferent from work minimal gaits. Nonlinear costs on force amplitude have similar results, in that they do not penalize jump discontinuities in the force profile (Figure 4.4, "force amplitude cost"). Therefore, in the context of walking, we believe considering costs for force amplitude production is less important than considering costs for force fluctuation, if mechanical work is also accounted for.

It is interesting to note that the optimization yielded some gaits with very little vertical excursion of the center of mass. Once thought to be an energetically economical strategy for human walking [35, 51, 76], experiments show a nearly level trajectory to be costly in terms of both metabolic cost and joint work [35]. The present model also finds it to be far from work-minimal, because high smoothness ($\alpha = 1$) requires that the legs produce opposing fore-aft forces, and hence work against each other through most of the stride. In pendulum-like walking ($\alpha = 0$), the legs perform no work except for the instantaneous support transfer, where vertical velocity is actively redirected upwards. This minimizes the time and amount of work of counteracting leg forces, but at the cost of very high forces and force rates (Figure 4.5). The addition of a cost for force fluctuation causes the redirection to begin before double support with a preemptive pushoff, and to end after double support when the leading leg completes a smoother collision. This bears closer resemblance to the redirection performed by humans [2]. The optimization illustrates the high cost of low COM excursions, and explains how the human preemptive pushoff phase can satisfy the trade-off between mechanical work and force fluctuation.

The optimization also discovers human-like vertical stiffness properties (Figure 4.7). Vertical stiffness summarizes overall oscillatory behavior in humans [46] and a wide range of animals [62]. Here, a cost for work tends toward infinitely high vertical stiffness for both walking and running (Figure 4.7), because high stiffness reduces displacement and therefore work. But with an increasing weight on force fluctuation, more displacement is acceptable because it allows decreased peak forces. As a result, the stiffness characteristics become more similar to human, for both single and (in walking) double support.

We found it curious that the optimization produces spring-like behavior (Figure 4.8), even though the model contains no springs. The spring-like gaits of humans are thought to take advantage of elastic tendons [32], which may reduce the active work required of muscle [4]. But considering that humans are not purely elastic, owing to contractile and dissipative tissues, we find it remarkable that they behave so much like ideal springs. Our model produces similar force profiles, despite having no elastic elements whatsoever. It is perhaps evidence that pseudo-elastic behavior is economical [74], regardless of actual elastic energy storage capability.

One consideration is whether the proposed objective function constitutes an actual

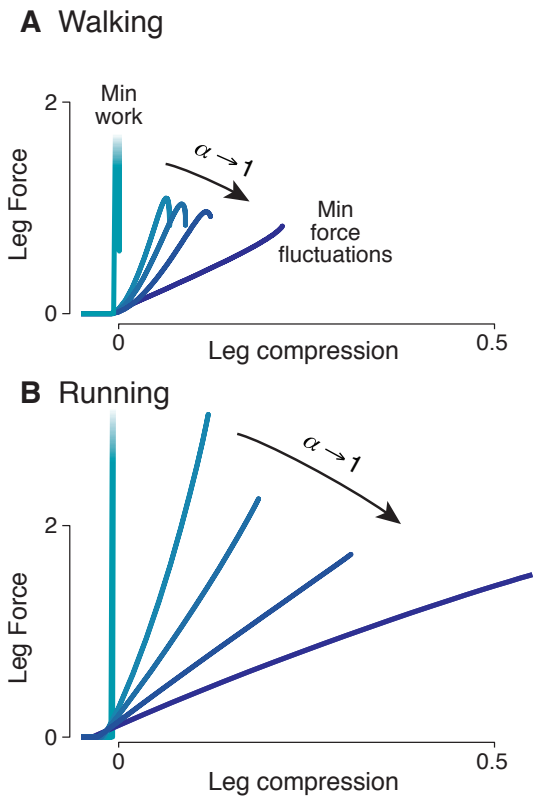

Figure 4.8: Leg stiffness of optimized gaits. Optimized leg forces versus leg displacements for walking (top) and running (bottom). Work optimized gaits approach infinite leg stiffness (slope of a linear fit to forces) during upward velocity redirection (roughly corresponding to double support in walking, contact phase in running). As the optimization cost includes a larger weighting α for force fluctuation, the optimal leg stiffness decreases for both walking and running.

metabolic cost. We based our objective J_f on an actual metabolic cost observed in periodic human motions such as moving the legs back and forth [24, 25] or bouncing vertically about the ankles [23]. Even accounting for work, humans expend additional energy to produce fluctuating forces, which appear to cost energy in part for cyclical activation (see e.g. [9, 42]). Our cost J_f is, however, only a crude representation rather than an accurate model of physiology. A sensitivity analysis suggests that even with variations in the force fluctuation cost's parameters, it still tends to produce rounded finite force peaks (Figure 4.3). The optimization is therefore sufficient only to demonstrate the effects of such a metabolic cost, without attempting to model it accurately. An optimization approach is unlikely to resolve the cost further without better experimental characterization of the underlying physiology.

The physiological cost of force fluctuation has been attributed to the pumping of cal-

cium associated with muscle activation and deactivation rather than shortening work [9,24]. It increases with movement frequency and amplitude [23], and therefore the impulsiveness of cyclical forces. The cost for activating muscle is associated with the number of contractions [9], or is combined with the cost of maintaining force [87], rather than the speed of changing forces. However, the experiments compared simple tetanus responses, while in arbitrary force profiles the number of contractions is less well defined. For example, a muscle exerting a sinusoidal force pattern of given amplitude would be expected to incur a calcium pumping cost for each dip in force. Increasing the frequency of the sinusoidal force output while producing the same amplitude would require more power to pump calcium, as the force dips are happening more frequently. This phenomenon can be roughly quantified by integrating the absolute value of the force derivative (or indeed any order derivative) during a period of interest. We propose that the integral of a force derivative-like term as a generalization of the number of muscle contractions for an arbitrary force profile. We therefore believe that the force fluctuation costs proposed in this study capture the costs of calcium pumping and help explain how humans choose walking forces.

It is also possible that humans favor less impulsive forces for reasons other than energy expenditure. For example, there could be a preference for lower peaks in force, simply to avoid pain or discomfort. Indeed, when landing from a jump, humans appear to modulate peak forces by bending their knees, even if that strategy costs them additional work to recover their upright stance [100]. It is possible that a similar preference could apply to locomotion. There may thus be other, non-energetic reasons why humans might avoid rapid force fluctuations. A general interpretation would be that humans prefer to locomote in ways that minimize a generic objective function that includes metabolic and non-metabolic costs, with metabolic costs including contributions for mechanical work and cyclical force production.

Yet another possibility is that the human-like forces are the result of neither cost nor preference, but limitations on body dynamics. The human body contains elastic tendons and deformable tissues [99], and therefore acts as a mechanical filter to reduce force peaks. But just as humans can modulate landing forces, they can also produce quite large peaks simply by landing with straighter knees [100]. Indeed we find humans to have little difficulty walking more rigidly, given simple instructions to do (Chapter 5). It therefore appears that humans could easily produce higher peaks than normally preferred, regardless of the body's mechanical filtering. Although that filtering is unavoidable to some degree, it also appears insufficient to entirely explain the relatively rounded, low-amplitude forces that humans typically prefer during locomotion.

There are a number of limitations to this study. We have examined an extremely simple

model of locomotion without many anatomical features. Our approach focused on avoiding additional parameters that a more complicated model would require, and instead focused on the basic requirements of bipedal locomotion. In addition, our cost function also only quantifies production of forces during stance. It does not place a cost on the swing phase, which may be especially unrealistic when the optimization yields a very long double support duration (Figure 4.5, "force fluctuation only") and an instantaneously fast swing. The inertia of the human leg limits movement speed [23, 24, 50], and evidence suggests a substantial metabolic cost for moving the swing leg [24]. That cost could also help to limit the duration of double support, which the present model determines based on stance phase forces alone. There may also be significant costs for maintaining balance or stabilizing the torso [23, 28], swinging the arms [19], counteracting torques about the vertical axis [19], walking at different step lengths [27] and widths [26] or for cushioning the body [99]. By constraining the nominal walking or running gait, we have effectively treated many such costs as constant. We propose that the production of work and fluctuating forces contribute significantly to the energetic cost of locomotion, but not to the exclusion of other costs.

Our model suggests that energetic cost may play an important role in determining human locomotion. The model further suggests that force amplitude is less important than force fluctuation when choosing forces in human walking, if mechanical work is also considered. Moreover, the components of energetic cost, such as for producing rapidly fluctuating forces, may help determine key aspects such as double support durations and rounded force peaks, as well as the resulting trajectory for the body center of mass. This implies that a system that uses actuators with different fundamental energetic costs, such as a walking robot with electric motors, or a human wearing an exoskeleton or rehabilitation device, might be expected to have quite different forces and kinematics if economy is important. Here, our model presupposes no pattern for ground reaction forces or kinematics, yet discovers human-like walking and running gaits, driven by hypothetical costs for work and force production alone.

4.5 Acknowledgements

This work was supported in part by Department of Defense (W81XWH-09-2-0142), National Institutes of Health (AG0308), and Defense Advanced Research Projects Agency (Atlas Program; Boston Dynamics, Inc.).

CHAPTER 5

The value of Smoothness in Human Walking

Human locomotion is governed in part by metabolic energy economy. Some aspects of preferred gait, such as step length, normally coincide with a minimum of energetic cost. Other properties of gait, such as ground reaction forces, are less clearly linked to energetic considerations. Previous simulation studies suggest that a cost for force fluctuation, but not amplitude, can explain the ground reaction forces seen in human locomotion, when combined with mechanical power. Here we explore a simple model of the energetic costs of using muscle, testing the cost of plausible walking force profiles. The model suggests that force profiles with more force fluctuation require increased calcium pumping costs. Based on these simulations, we hypothesize that human walking is determined in part by an energetically optimal tradeoff between mechanical power and force fluctuation costs. We perform an experiment to test this hypothesis by having human subjects walk with altered levels of force fluctuation in gait. We find that subjects expend more metabolic energy to walk with both reduced and increased force fluctuation (statistically significant using a paired wilcoxon signed rank test, 95% confidence). We attribute this metabolic power increase to a combination of mechanical work and force fluctuation. With reduced force fluctuation, the subjects walked with more mechanical power than normal, and with increased force fluctuation, the subjects walked with less mechanical work than normal. We attribute this observed tradeoff to an energetic optimization of mechanical work and force fluctuation, two costs of using natural muscle.

5.1 Introduction

Human locomotion is governed in part by metabolic energy economy. For a given speed, an individual's preferred gait normally coincides with a minimum of energetic cost [52]. As a result, alterations to variables such as the preferred stride length [27], stride width [26], and vertical displacement of the body [35], typically lead to increased energy expenditure. Since locomotion is powered by muscles, the metabolic energy cost associated with muscles must, in part, govern locomotion. Here we investigate the possible contributions of a basic cost of using muscles, that of changing muscle force, that might govern locomotion.

Energy is required to change the force produced by muscle. Artificial stimulation of a muscle with short pulses requires more energy expenditure than longer pulses, given the same overall stimulation time [9, 42]. Muscles primarily expend energy in two ways: crossbridge cycling to generate force, and pumping calcium, which regulates the amount of crossbridge cycling [7]. While crossbridge cycling can generate useable mechanical work (as well as isometric force), calcium pumping is a required additional cost that produces no mechanical work. This pumping process requires energy in the form of ATP hydrolysis. Furthermore, the rate of change of muscle force has been modeled with terms proportional to a normalized measure of calcium concentration (see [55], equation 36). Therefore, changing muscle force quickly might be associated with higher concentrations of calcium. Since pumping more calcium back into the sarcoplasmic reticulum costs more energy, changing muscle force rapidly may be more energetically costly than changing muscle force slowly. Tests of leg swinging provide further corroborating evidence for a metabolic cost of changing force in a muscle [24]. However, this muscle cost is generally overlooked when studying locomotion.

In rapid cyclic motion tasks, the delay caused by muscle activation dynamics hinders performance and potentially wastes mechanical energy [66, 89]. When driving a joint cyclically with the goal of maximizing speed, ideally a muscle would be at full activation while it is shortening, and at zero activation when it is lengthening. Any activation during lengthening would slow the motion, fight the antagonist muscle, and potentially waste energy. Due to activation dynamics, the activation level cannot change from zero to the maximum value, or vice versa, instantaneously, and therefore the timing of muscle stimulation must satisfy a tradeoff between producing maximal positive work and producing minimal negative work. It is possible that this effect will be evident in the spikey walking condition, but we do not measure the contraction of the muscles in the present study. However, we believe that normal walking does not require the subject to maximize the speed of a fluctuating joint, so we do not believe this effect will be the primary contributory factor to the

metabolic cost of walking with differing amounts of force fluctuation.

Metabolic cost estimates for muscles are used in the application of detailed human models to study locomotion. These models might, for example, be useful to study the role of muscle aging in locomotion performance [85]. Walking gaits for dynamic models of humans have been found [90] using an estimate of metabolic energy expenditure in muscles [10]. Experimental data can be fit to these models to infer physiological data which would be difficult to measure [45, 86], by minimizing total muscle activation based on empirical models of muscle force production and endurance [20]. None of the terms in the cost proposed are directly based on the fluctuation of the force, or on a jerk term (which would be proportional to a force fluctuation). Therefore, if a metabolic cost for changing muscle force exists, these detailed models of human locomotion may benefit from characterizing and including such a cost. One of our goals in this study is to determine whether a force fluctuation cost is relevant in human locomotion.

One approximation of metabolic power based on animal measurements is a rough relationship between body weight and the time of ground contact: $\frac{\dot{E}}{W_b} = \frac{c}{t_c}$, where $\frac{\dot{E}}{W_b}$ is the weight specific metabolic cost, t_c is the time of contact, and c is a constant, roughly 0.183 [48]. This relationship appears to hold for a wide range of animals and gaits, and arises from the proposal that producing forces to support body weight costs the majority of the energy required to locomote. Also cited is an observation that a metabolic cost for cross bridge cycling frequency could explain differences between metabolic expenditure in large and small animals [39] perhaps due to a difference in the muscle fiber type used (fast twitch versus slow twitch). We will investigate an alternative interpretation of the effect of muscle cycling costs on locomotion. We propose that a substantial metabolic cost can arise from increased muscle force fluctuation, without a substantial change in the contact time.

Simulations suggest that a combination of costs for mechanical work and force-fluctuation may explain the ground reaction forces seen in human walking (Chapter 4). One method that has been used to investigate the role of force fluctuation costs in human locomotion uses a very simple model of bipedal locomotion to find gaits that minimize a combination of work and a cost for changing forces. The model consists of a point mass pelvis and two massless, telescoping legs. Optimization methods were used to find leg forces that result in cyclic gaits at anthropomorphic walking speeds and step lengths. When finding gaits that minimize mechanical work, the optimization produces walking with perfectly rigid legs and impulsive leg forces at foot touchdown and toeoff [83]. This work minimal walking gait is also known as inverted pendulum walking since it can be produced by a semi-passive walker with rigid legs, where the body and stance leg act as an inverted pendulum, passively rotating in a circular arc about the foot on the ground for almost all of the

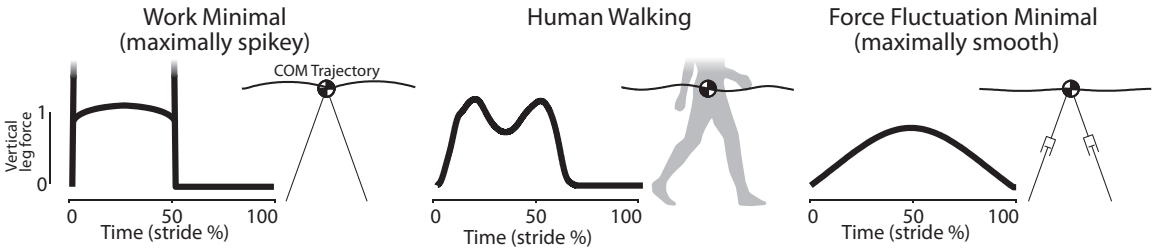

Figure 5.1: Comparison of idealized gaits and typical human walking. Optimization studies of a simple point mass model of walking suggest that minimizing mechanical work results in inverted pendulum walking (left), characterized by spikey, impulsive leg forces at heelstrike and toeoff, and a center of mass trajectory that follows circular arcs about foot placement locations. Toeoff occurs halfway through the stride, coinciding with heelstrike of the next leg (not shown), resulting in an instantaneously short double support period. When optimizing the same model to minimize a measure of force fluctuation (right), the resulting gait has smooth forces that gradually increase and decrease throughout the entire stride, resulting in an instantaneously short single support period when the massless leg is swung forward to the next step location. The center of mass trajectory follows a relatively flat trajectory. Human walking (middle) can be seen as a tradeoff between mechanical work and force fluctuation costs.

time (Figure 5.1). The only actuation is an impulsive pushoff from the trailing leg at toeoff, and an impulsive collision from the leading leg at heelstrike, which occur simultaneously, and together redirect the velocity of the hip mass onto an arc rotating about the new foot contact point. We refer to this gait as maximally spikey.

A cost for force fluctuation was then introduced to the optimization of this model. This cost was based, roughly, on the derivative of the force magnitude throughout the stride, which would result in a large cost for the work minimal, spikey gait due to the impulsive forces. When minimizing a combination of mechanical work and a cost for force fluctuation in the legs, walking is found with ground reaction forces exhibiting the smooth double peak characteristic of normal human walking, with roughly anthropomorphic double support periods and peak forces (Chapter 4). Further, minimizing force fluctuation alone produces a gait with very little vertical motion of the hip mass, along with single peak ground reaction forces and a double support period that spans the entire stride except for an instantaneous swing phase (Figure 5.1).

A number of other muscle costs were considered in previous walking optimization studies (Chapter 4). These included the time-integral of force, associated with isometric force production [40]. A nonlinearity factor was also considered based on signal-dependent noise [38]. Also, a simple peak force cost was considered, which might correspond to a physical limitation in peak force production. Each of the above costs was found to explain less of walking than a cost for force fluctuation.

Based on these simulations, we hypothesize that human walking is determined in part by an energetically optimal tradeoff between mechanical power and force fluctuation costs. We will test this hypothesis by measuring subjects walking with varying amounts of force fluctuation. We expect that spikey walking, with increased muscle force-fluctuation, will result in a decrease in the mechanical power used to walk, while smooth walking with decreased muscle force fluctuation will result in increased mechanical power. If humans naturally choose an energetically optimal gait, we expect that both spikey walking and smooth walking will require more metabolic energy expenditure than normal.

We will alter the amount of force fluctuation in gait by encouraging subjects to walk with reduced or increased double support period. Simple simulation studies of walking suggest that double support period changes with the amount of force fluctuation in the overall leg force in gait. In fact, if mechanical work is the only cost considered in walking, an instantaneously short double support duration is optimal. If force fluctuation is the only cost considered in walking, optimization suggests that the entire stride cycle should be spent in double support, with an instantaneously short swing phase. While neither of these gaits is feasible for a human, they suggest that force-fluctuation can be altered by modifying double support duration. We will then estimate the fluctuation of the ground reaction forces as a measure of muscle force fluctuation.

5.2 Methods

We estimated cost for calcium pumping based on an analysis of a simple Huxley model of muscle. Due to the time constants associated with cross bridge cycling, we believe there is a cost for changing force that, roughly, increases with the magnitude of the derivative of force. Combining the Huxley dynamic model of muscle crossbridge bonding with calcium activation dynamics (see [97], equation 5) yields a differential equation for the bond distribution n,

$$\frac{\delta n}{\delta t} = r([\text{CA}])fn - gn \text{ with "activation factor", } r([\text{CA}]) = \frac{[\text{CA}]^2}{[\text{CA}]^2 + \frac{k_{-1}}{k_1}[\text{CA}] + \left(\frac{k_{-1}}{k_1}\right)^2}. \tag{5.1}$$

The free calcium concentration is [CA], and f, g, k_1, and k_{-1} are timing functions associated with crossbridge bonding, crossbridge unbonding, calcium-troponin association, and calcium-troponin dessociation, respectively. Simplifying assumptions include isometric conditions and full crossbridge participation. We further simplify our analysis by considering f and g to represent simple time constants, and considering n to be proportional to

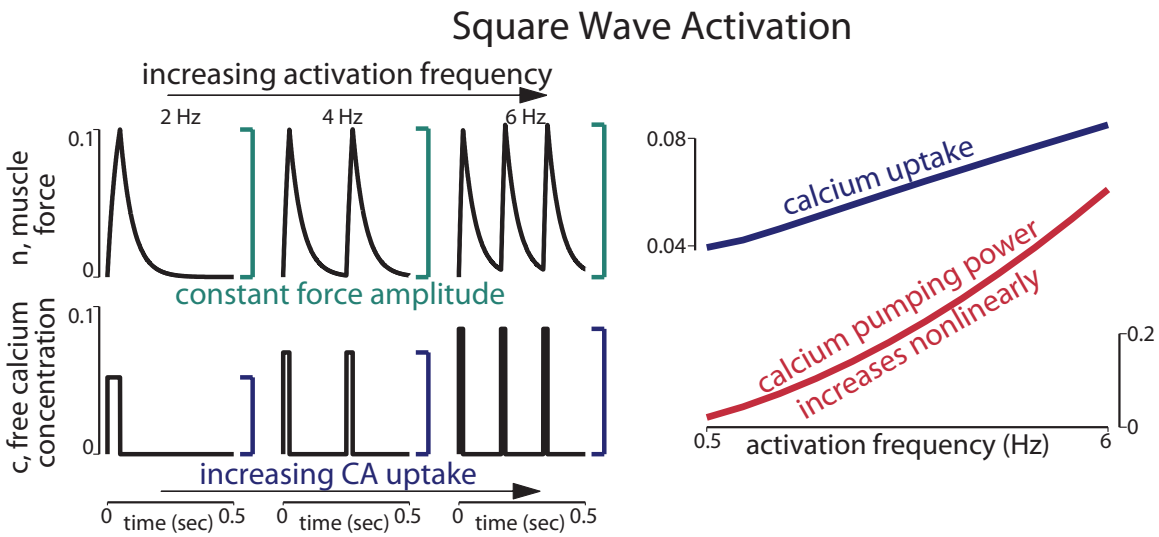

Figure 5.2: Model of required calcium pumping power in muscle with square wave activation. Computer simulations of crossbridge and calcium activation dynamics (Equation 5.1) driven by square wave calcium concentration activation (lower left), resulted in force force spike trains (upper left). A range of activation frequencies was tested, with a constant duty factor of 0.1. The amplitude of the calcium square wave was altered in order to keep the peak force produced constant across all activation frequencies. The amplitude of the square wave also represents the amount of calcium that must be taken back into the sarcoplasmic reticulum each cycle, which increases roughly linearly with frequency (top right). The power required to pump this calcium (calcium amplitude times the cycle frequency) increases nonlinearly with activation frequency (bottom right).

muscle force. To investigate the energetic consequences of pumping calcium into the sarcoplasmic reticulum, we performed a computational experiment using equations 5.1. We simulated the muscle with a square wave calcium concentration with an amplitude of $A_{[CA]}$, frequency $f_{[CA]}$ and a duty factor of 0.1. $A_{[CA]}$ was chosen to result in a reference peak force value. $A_{[CA]}$ is a measure of calcium that must be pumped into the sarcoplasmic reticulum per cycle, and multiplying by the frequency of the cycle, $A_{[CA]}f_{[CA]}$, yields a metric roughly proportional to the power required to pump calcium. Increasing $f_{[CA]}$ from 0.5Hz to 6Hz shows a greater than linear growth of the required power (Figure 5.2). This suggests that faster force fluctuations (e.g. larger $|\dot{\text{force}}|$) require nonlinearly more energy. To calculate $A_{[CA]}$, we simulated the activation and force generation dynamics (equations 5.1) for 1 cycle, using $f = \frac{1}{0.015sec}$ and $g = \frac{1}{0.05sec}$, [85], $\frac{k_1}{k_{-1}} = 0.2$ (see [96], Figure 9). The reference force peak amplitude was 0.1. To match peak force across frequencies an optimization routine (the fminunc function in MATLAB [59]) was used to optimize over $A_{[CA]}$ to minimize the difference between the reference force peak and the peak force simulated.

Previous studies have considered a simple cost for force fluctuation based on ground

reaction forces. The force fluctuation cost has the form

$$\text{force fluctuation} = \frac{\sum_{i=0}^{N_{\text{stride}}} \left(\int_0^{t_{\text{stride,i}}} \left| {f^{(n)}}_i \right|^p dt \right)^{\frac{1}{p}}}{N_{\text{stride}}}, \tag{5.2}$$

and penalizes faster changes in force, as they require larger changes of calcium concentration. $f^{(n)}$ is the n^{th} derivative of the magnitude of the leg force. This measure roughly captures the idea of a cost for calcium uptake demonstrated above (Figure 5.2) which increases nonlinearly with the rate of change of force production. A modelling study considering equation 5.2 as a cost for a walking model, discovered ground reaction forces for walking with varying amounts of force fluctuation, but constant walking speed and step length (Chapter 4). Here we consider the calcium concentrations required to produce those forces, and the corresponding cost of calcium uptake during these walking gaits. The ground reaction forces from the modelling study (scaled by a factor of 0.1) (Figure 5.3, muscle force, dashed lines) are taken as target force trajectories. A trajectory of calcium concentration through time was calculated (Figure 5.3, free calcium concentration) which resulted in forces (Figure 5.3, muscle force, solid lines) most closely matching those from the modelling study. Calcium uptake for each condition was calculated as the sum of the calcium differences from peaks to troughs of the calcium concentration trajectory. We expect these dips in calcium concentration to occur due to uptake of free calcium into the sarcoplasmic reticulum, and therefore require energy expenditure. The power required to pump the calcium was calculated by dividing by the step time (constant across conditions). As expected, the pumping power increases as the gait includes more force fluctuation, as measured by equation 5.2. Physiological experiments would be required to more carefully characterize values of the force fluctuation derivative order n and nonlinearity factor p.

5.2.1 Experimental protocol

Subjects walked under conditions designed to alter the amount of force fluctuation in their muscle forces. Subjects first walked on a treadmill to obtain baseline walking (1 minute) and their ground reaction forces were recorded. The baseline average stride (T_{baseline}) and double support ($\text{DS}_{\text{baseline}}$) durations were calculated using the vertical ground reaction forces.

We collected three experimental trials: normal, spikey, and smooth. During these trials, subjects were shown visual feedback, representing a gait cycle over time, with a blue rectangle where left foot ground contact was desired, and a red rectangle where right foot contact was desired, with purple representing double support. The vertical components of

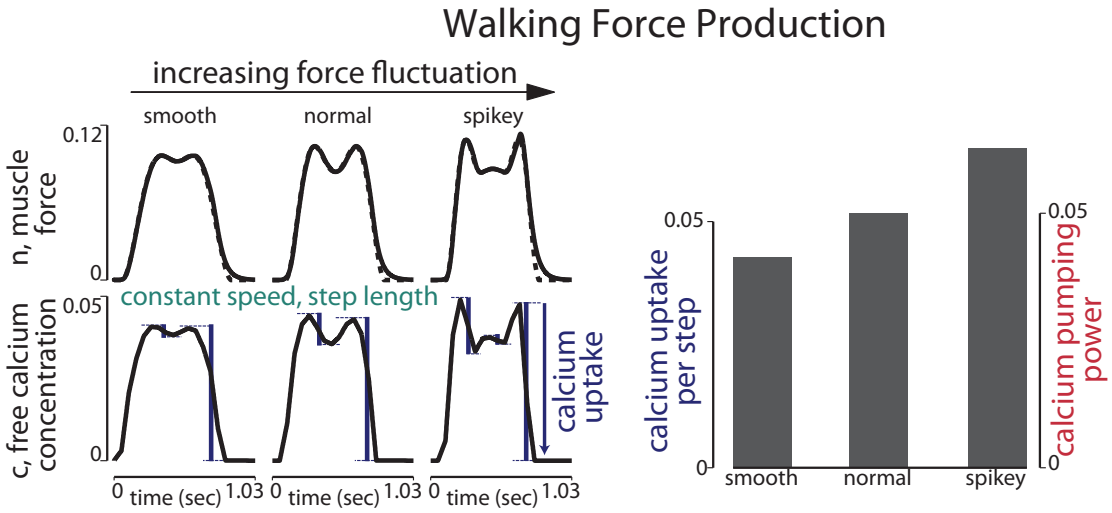

Figure 5.3: Model of required calcium pumping power in muscle producing walking forces. Numerical optimization is performed to calculate the required calcium concentrations (lower left) that result in muscle forces (upper left, solid) that correspond most closely with ground reaction forces of simulated walking (upper left, dashed), given the model of crossbridge and activation dynamics of Equations 5.1. The simulated walking forces are taken from a simulation study of walking at constant speed and step length (0.4 and 0.68, respectively), but with varying amounts of "force fluctuation". Any drop in the calcium concentration is assumed to be a result of calcium uptake into the sarcoplasmic reticulum, and therefore energetically costly. Increasing force fluctuation results in increasing calcium uptake per step, with a corresponding increase in average power attributable to calcium pumping (right).

the left and right feet were overlayed on the desired contact periods as blue and red lines, respectively, which updated in real time from left to right. At the end of the stride cycle (T_{baseline} for all conditions), the lines wrapped around and began updating at the beginning of the stride cycle. Subjects were asked to walk (6 minutes) such that the blue and red lines were greater than zero in the blue and red regions, respectively, with both above zero in the purple regions. The distinguishing factor between the normal, spikey, and smooth conditions was the width of the desired double support region, which was $\text{DS}_{\text{baseline}}$, $\text{DS}_{\text{increased}}$, and $\text{DS}_{\text{reduced}}$, respectively. Ideal subject performance would result in the same stride frequency across all conditions.

Before the smooth (increased double support trial) walking trial, the subject was instructed to walk "sneaky" by bending their knees and crouching over while leaning slightly forward. Before the spikey (decreased double support) walking trial, the subject was instructed to walk while keeping their legs straight and their back rigid, keeping their weight more on their heels. In pilot testing, these instructions appeared to result in more reliable changes in force fluctuation than visual feedback alone. In addition, subjects walked for a short period until they appeared to reach a steady gait before data collection was begun.

Subjects walked on a split belt force-instrumented treadmill (Bertec). Motion capture markers were used to record the motion of the lower body (Phasespace). Subjects also wore a respiration sensor (Oxycon Mobile) to measure metabolic energy expenditure. All trials were performed at 1.25 m/s. 9 subjects were tested, (5 female, with age mean and standard deviation of 21.2 and 2.4 years, respectively). Forceplate and motion capture data were taken for 60 seconds, at the beginning of the 6 minute walking bout. Due to instrumentation problems joint mechanics, center of mass mechanics, and metabolic data are available for 6, 8, and 6 subjects, respectively.

5.2.2 Outcome Measures

To quantify subject performance in the walking task, we compared aspects of gait to ensure that the conditions represent walking with differing levels of force fluctuation. In the smooth walking condition, we expected the peak vertical ground reaction force and force fluctuation to be reduced with respect to the normal walking case. Similarly, in the spikey condition, we expected the peak vertical ground reaction force and force fluctuation to be increased with respect to the normal walking case.

To quantify the force fluctuation of gait, we will use equation 5.2, with $n = 1, p = 3$ for this experiment. Force fluctuation was calculated using the left leg ground reaction force, filtered with a butterworth filter (3rd order lowpass, 100Hz cutoff frequency). It was

calculated for each step individually, then averaged over all strides. This avoids any filtering of rapid force changes that would result from averaging all strides before calculating force fluctuation.

To assess the energetic effect of walking with differing amounts of force fluctuation, we quantified several measures of energy expenditure. First, to estimate metabolic expenditure, we averaged the volumetric flow rates of respiratory gases over the last three minutes of each walking trial and calculated the metabolic energy cost based on the relationship between exchanged gases and chemical energy [1, 15].

In addition, we quantified the overall power performed on the center of mass over a stride. We first averaged the left and right leg forces (assuming left/right symmetry). We computed the dot product of the ground reaction force of one leg with a center of mass velocity estimate, yielding average power a leg performs on the center of mass [29]. We then calculated the average over time of the absolute value of the power curve. This was doubled to find the center of mass absolute power.

Finally the mechanical power performed by the joints was calculated based on the motion capture data and force plates using standard software (Visual3d, C-Motion, Germantown MD, USA) [99]. We filtered the forces and motion capture data (butterworth lowpass filter, cutoff frequency of 6Hz) to reduce noise. We then calculated joint angles, moments, and powers for the ankle, knee, and hip, and averaged them over strides. We calculated the average of the absolute value of the power curve of each joint, and summed these to quantify average absolute joint power.

Our analysis was performed by calculating average quantities across strides. We demarcated strides using the vertical force. Assuming steady walking, the data over each stride were interpolated and averaged together to yield the average curve for the subject. Furthermore, we assumed left/right symmetry, so the averaged data associated with the right leg were shifted in time by half the stride period and averaged with the data from the left leg. However, we performed no averaging when calculating the force fluctuation measure, which is sensitive to the smoothing that comes from averaging. To perform statistical analyses, all quantities were non-dimensionalized using leg length, body mass, and gravity as base units.

To quantify differences between conditions, we tested whether outcome measures across subjects change from the normal condition. Pilot testing suggested that, given the subjective aspect of the conditions, a normal distribution might poorly model the subject's outcome measures. Therefore, to test the effect of condition on a given summary measure, a paired Wilcoxon signed rank test was performed [34], in lieu of a T-test. This tests whether the median change from normal across subjects is significant against the null hypothesis

Condition	Stride Length	Stride Length RMS	Stride Speed	Stride Speed RMS
Spikey	1.43 ± 0.0495	0.057 ± 0.0216	0.412 ± 0.0126	0.0079 ± 0.00164
Normal	1.45 ± 0.0607	0.0445 ± 0.0189	0.414 ± 0.013	0.0072 ± 0.00213
Smooth	1.45 ± 0.0556	0.0743 ± 0.0373	0.413 ± 0.0123	0.0137 ± 0.0122

Condition	Double Support Duration	Double Support Duration RMS
Spikey	0.468 ± 0.0419	0.0261 ± 0.00734
Normal	0.502 ± 0.0321	0.0228 ± 0.00402
Smooth	0.483 ± 0.0255	0.036 ± 0.0101

Table 5.1: Walking parameters during experimental conditions. Parameters are averaged across all subjects (mean $\pm$ standard deviation). All parameters are nondimensionalized by leg length, body weight, and gravity.

that there is no change in the median. This test assumes the data are drawn from a symmetric, but not necessarily normal, distribution. Tests for significance are performed at a confidence of 95%.

5.3 Results

The vertical ground reaction forces of a representative subject exhibits higher peaks and lower contact duration in the spikey condition than normal (Figure 5.4). The smooth walking condition exhibits less force fluctuation overall (lower peak force and more constant force during mid stance). The joint powers averaged across all subjects (calculated from joint angles and moments, (Figure 5.5)) show more negative ankle work in the smooth condition than normal walking, while spikey walking exhibits less positive ankle work during pushoff. In addition, spikey walking exhibits less knee work at the end of the swing phase than normal.

Subjects exhibited significantly more metabolic power in both spikey and smooth walking with respect to normal (Figure 5.6). Spikey walking was found to exhibit significantly less absolute joint power than normal, and more force fluctuation than normal. Smooth walking exhibited significantly more absolute joint power than normal, and less force fluctuation than normal. In addition, spikey walking exhibited more power estimated by a simple contact time relationship [48] than normal, but smooth walking did not.

Shown in table 5.1 are walking parameters for the various conditions. Higher variability is evident in the smooth and spikey conditions, possibly due to the difficulty of maintaining these abnormal gaits.

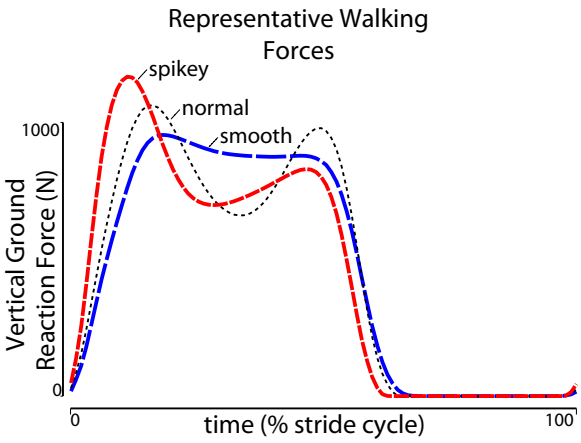

Figure 5.4: Vertical ground reaction forces for a representative subject. Shown are ground reaction forces for one leg (average of left and right legs for all strides). The spikey condition shows a higher peak collision force than normal, and the smooth condition shows a slower rise and decay in force than normal, as well as less fluctuation than normal in mid stance. Contact time is slightly shorter than normal in the spikey condition and slightly longer than normal in the smooth condition.

5.4 Discussion

Our findings are consistent with the theory that preferred walking involves a tradeoff between the metabolic costs of force fluctuation and mechanical work. As expected, when asking subjects to walk with increased or decreased force fluctuation, metabolic cost was higher than in preferred walking. Decreased force fluctuation was associated with more mechanical joint work, in agreement with previous experimental [35] and simulation studies (Chapter 4). This is consistent with an increase in metabolic cost for mechanical work with a smaller decrease in metabolic cost due to force fluctuation. When walking with increased force fluctuation, mechanical power decreased with respect to normal walking, in agreement with previous simulation studies (Chapter 4) and therefore mechanical power cannot explain the observed increase in metabolic expenditure. However, considering an additional metabolic cost for changing muscle force, which is well documented at the level of a single muscle, can explain the additional energy expenditure observed.

The decreased mechanical power associated with increased force fluctuation walking appears to be due to reduced positive pushoff work from the ankle (Figure 5.5, Ankle Power) and reduced negative knee work in late swing (Figure 5.5, Knee Power). The decreased knee work in the spikey condition might be due to a straighter leg during swing, with less angular excursion (Figure 5.5, Knee Ankle). This suggests that the swing phase can have a substantial impact on the energetic requirements of gait, which have been ignored when deriving simple relationships between metabolic cost and contact time [48], as

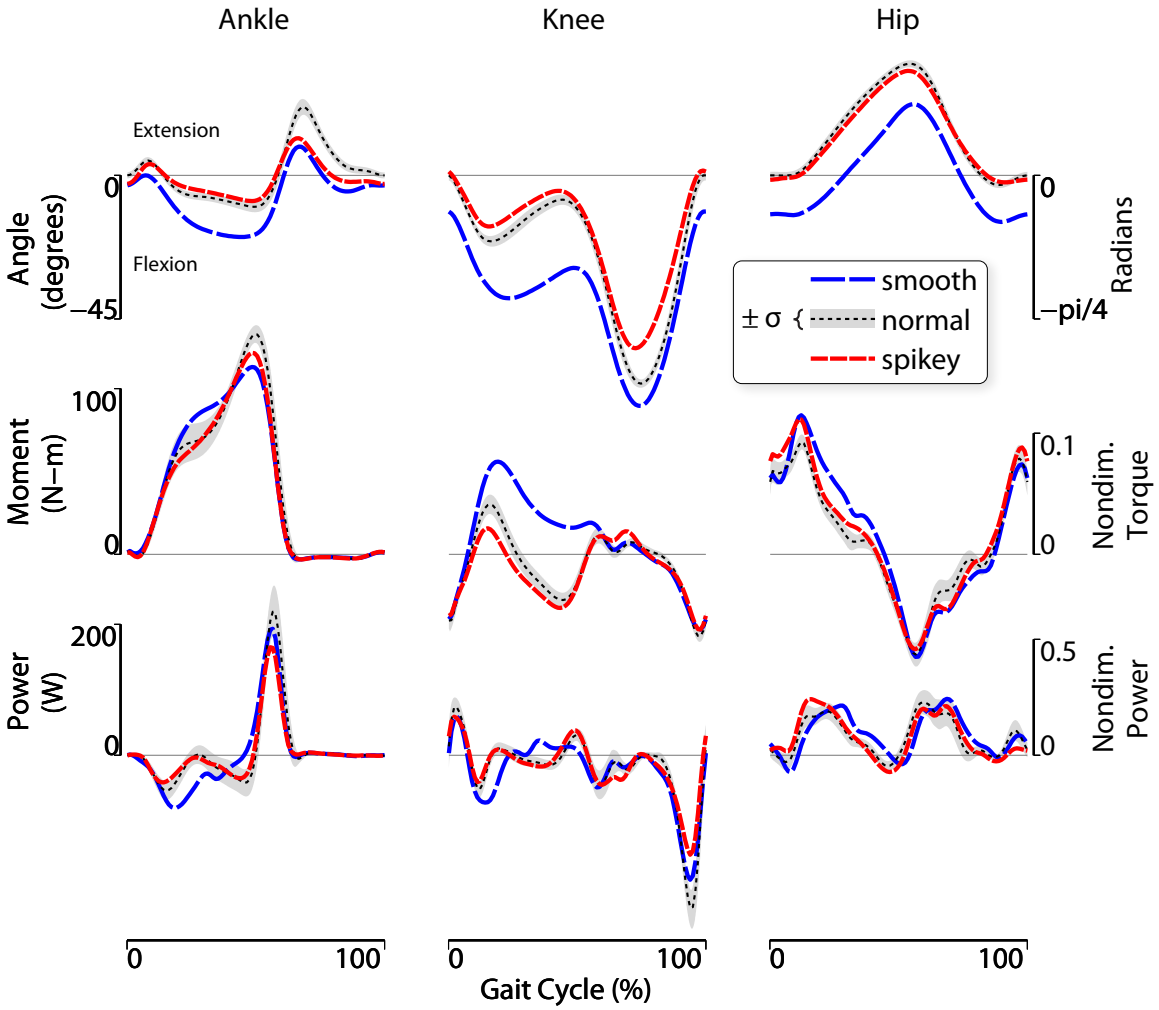

Figure 5.5: Average joint kinematics, moments, and powers, for all subjects and conditions. Joint angle (top row), moment (middle row), and power (bottom row) are shown for the ankle joint (left column), knee joint (middle column), and hip joint (right column). Only the saggital plane components are shown for angle and moment. Note smaller absolute peak power for the ankle and knee joints in the spikey condition. There is also more negative power of the ankle joint during stance in the smooth condition. The gait cycle shown begins at the heelstrike of the leg shown. All angles are shown with zero defined as the averge initial angle of the normal walking condition.

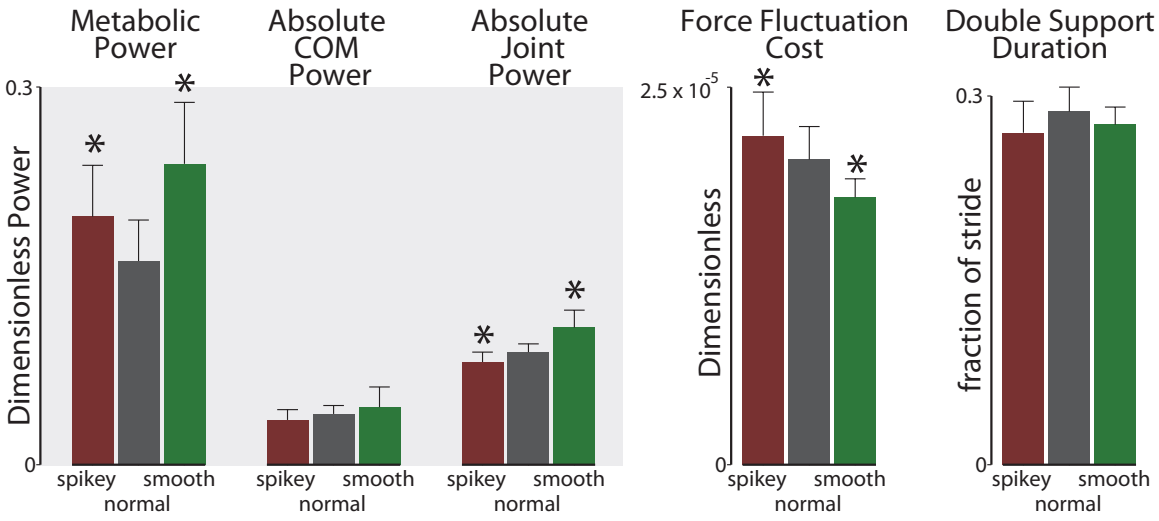

Figure 5.6: Summary measures averaged across subjects: estimates of power (metabolic, center of mass, joint), force fluctuation cost, and double support period. Vertical bars denote 1 standard deviation. Asterisks denote significant difference from the normal condition at the 95% confidence level using a paired Wilcoxon signed rank test. Meaures were nondimensionalized for each subject before averaging, using leg length, body mass, and gravity.

well as in our previous simple models of force fluctuation cost (Chapter 4).

One limitation of the present study is the imperfect estimation of mechanical power generated by the muscles. Mechanical power is quantified in two ways, center of mass power and joint power. Center of mass power quantifies the overall power performed by the legs on the center of mass. This measure might include factors such as soft tissue deformation, for example passive oscillation of viscera [99], which have no direct metabolic consequence. On the other hand, center of mass power fails to capture so-called peripheral, or internal, power, which results when forces internal to the body perform work in such a way that it does not affect the center of mass dynamics (for example symmetric oscillations of masses about the center of mass) [18, 100]. Peripheral power might be metabolically costly, but is not measured by center of mass power. The other estimate of mechanical power exerted by the body is joint power. Joint power was calculated using commercially available software, which combines ground reaction force measurements with kinematic information of the body to estimate the moments and powers developed at each joint. Both center of mass and joint power include elastic tendon power, which is performed passively, and therefore need not be generated by muscle [100]. Despite the limitations in the measurements, we believe they roughly describe the mechanical power performed by the relevant muscles in gait.

Another limitation of this study is the approximate estimation of the cost of force fluc-

tuation in muscles. Generally, we propose the cost of force fluctuation only as a rough approximation of the actual metabolic cost of changing the force of a muscle. The force fluctuation metric we calculate is based on the ground reaction forces, which result from the combined contributions of many muscles, as well as passive elements such as tendons and other soft tissue. In a holistic activity such as walking, force fluctuation cannot be easily separated from other potential basic muscle costs, such as simply producing force. Despite the approximate nature of the metric, we consider force fluctuation a plausible explanation for the metabolic energy cost changes observed in this study.

A further limitation of this study is the experimental methodology employed to elicit force fluctuation changes. Subjects appeared to have difficulty steadily walking with force fluctuation levels differing from normal walking (Table 5.1). While the measured force fluctuation levels changed as predicted (based on a statistical analysis, Figure 5.6), it is possible that additional training, or more effective feedback, could result in more reliable changes in force fluctuation. This may improve future studies of the role of force fluctuation in gait.

Another limitation with the current study is the simplified model on which the hypothesis is based. There is an asymmetry in the proposed walking model with respect to the experimental conditions. The reduced force fluctuation model represents the legs as massless sliding joints, whereas a human approximates the reduced force fluctuation center of mass trajectory by significantly flexing the knee. The thigh and shank have significant rotational inertia, and the sliding leg neglects these dynamics, so a human walking with reduced force fluctuation acts less like the model. On the other hand, the spikey condition is an attempt to approximate a model with rigid legs, so the human may act more like the model.

We do not believe a simple relationship between contact time and energy expenditure can explain the results found in this study. The estimated power from contact time is significantly higher than normal in spikey walking, while no significant relationship is found for the smooth walking condition. However, the measured metabolic power was higher than normal in both the spikey and smooth walking conditions. We propose that the relationship between energetic expenditure, body weight, and contact time found in a wide range of animals of different sizes and preferred gaits [48], is a result of a tradeoff between metabolic costs for mechanical work and muscle force fluctuation.

Our findings are consistent with the theory that preferred walking involves a tradeoff between the metabolic costs of force fluctuation and mechanical work. When asked to walk with increased force fluctuation, subjects walked with decreased mechanical power but increased metabolic power. Previous estimates of metabolic expenditure attempting to

capture the relationship between force production frequency and energetic expenditure fail to explain the results found. In addition, our findings disagree with previous theories on the energetic efficiency of walking with a flat center of mass trajectory. A combination of costs for producing mechanical work and force fluctuation can explain the observed increased metabolic cost of walking with decreased mechanical power. We believe that motions powered by natural muscle involve a tradeoff between the metabolic cost of producing mechanical work with the metabolic cost of changing the muscle force.

CHAPTER 6

Concluding Remarks

In this work we have explored mechanisms of stability and metabolic cost in human walking. The underlying basis for this work is the use of simple dynamical models and control systems tools. The models have been applied to the development of engineering methodologies, particularly to state estimation from inertial measurement data (Chapter 2) and controller design for walking (Chapter 3). Models have also been used to address scientific questions regarding human locomotion, for example to determine the variability of human footfalls during overground walking, and then to the structure of those footfalls and the relation to stability. I also applied modeling to explore candidate optimization costs that might govern the basic force profiles produced by the legs during locomotion, accompanied by a human subjects experiment that demonstrates the possible outcomes from such costs. Here I summarize these results in terms of engineering and scientific contributions, followed by discussion of limitations as well as possible future applications.

An engineering challenge associated with locomotion is the hybrid nature of the dynamics. Locomotion entails discrete events (e.g., heelstrike impact) acting on continuous-time dynamics, and the resulting nonlinearities make it challenging to analyze stability and design controllers and estimators. In the case of state estimation, I treat the discrete event as an advantage: each stance phase enables drift correction of inertial measurement data, so that data need only be integrated over the relatively short continuous-time interval of a single swing phase. Compared to continuous integration without the periodic correction, my proposed estimation method performs with orders of magnitude improvements in accuracy.

I adopt a straightforward approach for the design of controllers. I treat each heelstrike event as a Poincare section, so that the overall step-to-step dynamics may be modeled as a discrete time system. Linearizing that system, each step allows for computation of a control law, based on standard control design methods (e.g., pole placement), that commands a feedback correction that must then be implemented in continuous time. For example, the adjustment of foot placement and foot heading could then be performed during a swing phase, and thus continuous- and discrete-time control can complement each other for the

overall maintenance of balance. This finding is easy to understand and directly suggests experiments that can be performed on human subjects.

This approach contrasts with other, highly sophisticated computational tools for designing hybrid system controllers (e.g. [92]). Those tools certainly have advantages with regard to complex systems, but they are also less amenable to engineering reasoning. One might expect a nonlinear system controller to optimally control foot placement and heading in a coupled manner as I have proposed. But the analysis of many degrees of freedom and many states would not necessarily make the coupling as clear and intuitive as my analysis. For answering simple questions such as what degrees of freedom are sensible for a robot, it may be helpful to use simple models to reveal physical behaviors that might be harnessed for control. I propose that simple models remain useful even in the presence of powerful but more complex methods.

I believe my approach is especially amenable to scientific inquiry. I have used a simple model of 3D locomotion to propose the hypothesis the humans might steer the foot like a bicycle wheel to maintain lateral stability. I performed a human subjects experiment that demonstrates a coupling between foot placement and heading that agrees well with the model prediction. A separate and even simpler model was applied to the optimization of locomotion. Whereas a previous study demonstrated how minimization of mechanical work could determine basic features of force profiles during locomotion, they also failed to explain the rounded shape of actual human forces. My models show that a single additional cost, related to fast fluctuations in forces, can explain the forces produced during both walking and running. I also performed a human subjects experiment that demonstrates a metabolic cost for locomotion that cannot be explained by mechanical work, but can be explained by the proposed cost.

There are, of course, limitations to this simple modeling approach. Simple models must be constructed carefully so that they include only the simplest features necessary to capture the phenomena under study. It is always possible that a more complex walking model will produce a different explanation. However, the simpler model is easier to interpret, and, if it does capture the most fundamental aspects of locomotion, is likely to be more generally useful. We now consider further implications for this work, both in clinical populations and in robotic applications.

6.1 Implications for clinical populations

This work may have implications for clinical populations, such as those that walk with prostheses or orthoses. Our finding that foot heading is used in stabilizing healthy human

gait warrants consideration in the design of devices used to assist walking, particularly as falls are likely [64]. Similarly, our finding that force fluctuation is a significant determining factor of the energetics of walking should be considered when serving populations that already have reduced metabolic economy [91]. We now consider possible implications for these findings in trying to improve the design of prostheses and orthoses.

The finding that foot heading can be used to stabilize gait (Chapter 3) may have potential impact on the design of prostheses or orthoses, which currently may limit the ability of a patient to alter foot heading on a step to step basis. For example, an active ankle prosthesis could detect a wider stride width than normal using inertial sensors, and react by rotating the foot externally. This may lead to improved stability if it correctly simulates what people choose to do with natural ankles. A hip orthosis could similarly provide a coupling between foot placement and pelvis heading. It is also possible that this coupling, present in healthy subjects, is imparied in subjects likely to fall. More research would be required for any particular patient population, but it is possible that an impaired ability to finely control yaw rotation of the foot would remove one mechanism of balance and lead therefore to more falls.

I furthermore found that the ground reaction forces in walking are determined more by the metabolic cost of changing force than maintaining force. This may have implications for prosthesis design, as amputee walking general suffers poorer energetic economy than intact subjects. Prostheses designed to perform pushoff work to reduce the metabolic cost of walking might also need to consider any sharp forces exerted, as these forces may have to be counteracted by the subject's muscles. For eample, if a prosthesis provides a sharp, strong pushoff impulse at toeoff, the subject might activate the hamstring muscles rapidly to avoid excess knee flexion. This activation may require little mechanical work, but if done quickly may require significant energy for activation.

In addition to these scientific results, I presented a technical contribution for measuring natural gait outside of a laboratory environment (Chapter 2). Commercially available hardware allows the capture of inertial data over entire waking day periods, allowing long term monitoring of gait. Experiments are being carried out using these techniques to measure frail elderly subjects for week long periods. In addition, we have used inertials gait monitoring to capture gait in natural environments, such as on rough outdoor terrain, marathon running, and mountaineering. We are also integrating inertial sensors into active prostheses to better sense and react to user intent. The ability to capture step placement in spontaneous walking outside of lab may also provide insights into how gait changes throughout the day or from day to day.

6.2 Implications for the stability and energetics of robotic walking

In addition to clinical populations, I believe this work can have applications to artificial walking, such as humanoid robots. To have a humanoid operating safely, a stable gait is required to avoid falling and possibly injurying users or damaging the robot. In addition, if a machine is to carry its own power source to increase mobility over tethered robots, energy economy is a valuable gait property.

The inertial sensing method described in this thesis (Chapter 2) could in principle be applied to any form of legged walking. Applying the methods described here can provide an estimate of the robot's trajectory from each foot for use in control. In addition, mounting inertial sensors on the feet of legged robots would be particularly useful to detect any slip conditions in the stance foot, which is otherwise difficult to detect with encoders alone. Inertial sensors are also particularly good at detecting if the foot has hit an unexpected obstacle, since impacts register as spikes on the accelerometers. Inertial sensors also estimate orientation and angular velocity in a gravity referenced frame, which complements the relative orientation estimates from encoders.

In addition to the technical contribution to sensing robotic systems, robots could use foot steering (Chapter 3) to walk with increased stability. In particular, given a large lateral disturbance, if step placement is insufficient (particularly if the robot leg is speed-limited and cannot step out in time to recover), adding a change in foot heading may avoid a fall. This ability has implications for the structure of controllers. One control approach is to decouple control of various aspects of the robot in order to achieve desired behavior for them. One famous example is Raibert's hoppers, which independently controlled body attitude, hopping height, and forward speed. This approach works well when the phenomena under control are relatively decoupled from each other and can be stabilized independently. One result from the foot heading model is the coupling between lateral balance and yaw. Therefore, it is likely detrimental to stability to design a control module for balancing the robot and seperately design a higher-level control module for global heading. A controller that simultaneously accounts for any balance needs while performing higher-level heading corrections with lower priority would likely be more successful, if more complicated.

We optimized a simple model of walking to study the tradeoff between mechanical work and a low level muscle cost in human walking (Chapter 4), but this method could just as easily explore efficiency in robot gaits. Electric actuators, for example, do not generally require significant power to change force, so we might expect a different energetically optimal gait for an electrically powered humanoid robot than for a human. If the cost

of using an electric motor is a combination of mechanical work and torque maintenance (motor current times internal resistance), we would expect a force amplitude production cost function. Since the walking model applies equally well to humans, humanoid robots, or any other bipedal locomotor, we can apply the energetically optimal trajectories for force amplitude costs to an electric robot. We would therefore expect an energetically optimal gait to resemble inverted pendulum walking with clipped peaks (Figure 4.3, amplitude force costs). There are other considerations in robot gait, just as in human walking, such as actuator bandwidth limitations and impact considerations for safety. However, we believe that the results from the proposed simple model could be used as a first order approximation of minimizing energy based on fundamental energy costs.

Simple mechanical models have further implications for robotics, such as for use in path planning. It is likely that humans are a good source from which to learn about walking, so anthropomorphic control properties might be a good starting point for a stable and efficient robotic controller. One of the results of experimenting on human gait using simple models is a family of models that capture the dynamics of human locomotion. These models can then also be used to solve other problems in robotics, such as path planning. Path planning for complex systems often suffer from a curse of dimensionality. It is possible that an optimal path, or an optimal controller, or an optimal state estimator, for a simple model that captures the natural dynamics of walking will be a good starting point for a path, controller, or state estimator for a more complicated physical robot. Optimal controllers for simple models may not necesarily result in optimal controllers for a real robot, but they are likely a good first step towards robust walking robots that can operate safely for long periods of time outside of lab environments.

6.3 Remarks on the use of modeling

This thesis has focused on the stability and energetics of human walking, using simple modelling. Human walking is a complex activity, and it is often difficult to attribute measurable aspects of walking (such as the ground reaction forces, or foot placement variability), to anatomical features or desired goals of locomotion. However, some underlying principles of locomotion such as stability and energetic efficiency can be studied using simple models with few parameters. Using simple models allows testing hypotheses in an isolated system. It is relatively straightforward to model the dynamics of rigid body linkages, as opposed to, for example, the complexities of natural muscles connected via tendons to bones. Therefore it is easier to interpret results of experimentation on simple mechanical models, as the only possible explanation must be based on mechanical principles. Like all models,

however, mechanical models can only be used to explore phenomena they capture. For example, the correlation between stride width and foot heading might be explained using an argument not based on stability. However, we believe that stability and energetics are fundamental principles underlying gait, and we will generally attempt first to explain observed phenomena in gait using such fundamental principles.

APPENDIX A

Work-Force Optimization Process

Here we provide details of the optimization of work and force costs in walking used in Chapter 4. At evenly distributed times in the trajectory, $i \in [1...N]$, we define body positions ($\vec{p}_i = (x_i, y_i)$), and velocities ($\vec{v}_i = (\dot{x}_i, \dot{y}_i)$), and the force magnitudes along the leading and trailing legs, (f_i and $f_i^{'}$, respectively). We perform an optimization of all of these variables throughout the step,

$$C := \left[\begin{array}{cccccccc} \vec{p}_1 & \vec{v}_1 & f_1 & f_1^{'} & ... & \vec{p}_N & \vec{v}_N & f_N & f_N^{'} \end{array} \right].$$

The optimization routine (a sequential quadratic programming algorithm, the MATLAB fmincon function [59]) searches over C, minimizing the cost function (J) while satisfying the following constraints.

A multiple shooting integration approach is used to constrain the state trajectory to be dynamically feasible. Defining force vectors along the leading and trailing legs as

$$\vec{f}_i := f_i \frac{\vec{p}_i}{||\vec{p}_i||} \text{ and } \vec{f}_i^{'} := f_i^{'} \frac{\vec{p}_i + (L_{\text{step}}, 0)}{||\vec{p}_i + (L_{\text{step}}, 0)||},$$

each state in the trajectory is constrained to be equal to the previous state integrated forward over a time period Δt, ($\Delta t = T_{\text{step}}/(N-1)$), satisfying the differential equations $(\ddot{x}, \ddot{y}) = \vec{f} + \vec{f}^{'}$, where $\vec{f}$ and $\vec{f}^{'}$ are linearly interpolated between forces at the control points, $\vec{f}_i$ and $\vec{f}_i^{'}$, respectively. The integration is performed using a fixed step Euler method. To improve the stability of forward integration, we apply 20 intermediate steps between each control time step Δt.

Additionally, the leg force is constrained to be zero at the beginning and end of a stride, $f_1 = 0$, and $f_N^{'} = 0$. The gait is constrained to be a limit cycle of locomotion by constraining the final state of the body mass to be equal to the initial state translated forward by the

nominal step length,

$$\begin{bmatrix} x_N + L_{\text{step}} \\ y_N \\ \dot{x}_N \\ \dot{y}_N \end{bmatrix} = \begin{bmatrix} x_1 \\ y_1 \\ \dot{x}_1 \\ \dot{y}_1 \end{bmatrix}$$

Finally, each leg is constrained to exert zero force if the foot is not on the ground (i.e. the distance between the body and the foot's nominal location on the ground is greater than the maximum allowable leg length, 1),

$$\begin{aligned} f_i &= 0 \quad \text{if} \quad ||\vec{p}_i|| > 1, \text{and} \\ f_i^{'} &= 0 \quad \text{if} \quad ||\vec{p}_i + (L_{\text{step}}, 0)|| > 1. \end{aligned}$$

To improve the numerical behavior of the simulation routine, we use an approximate absolute value function when calculating the cost, $|x|_* = \sqrt{x^2 + \epsilon^2} - \epsilon$, with $\epsilon = 1 \cdot 10^{-7}$, which eliminates the first derivative discontinuity of the absolute value function at zero. In theory this approximation does not change the optimization results since both the absolute value function and this approximate function have a single minimum at zero.

The initial guess for body trajectory was a constant height of 1, a steady forward progression at the nominal speed. The initial guess for leg forces was half body weight with a small amount of added random noise. To ease the optimization problem and test for discretization effects, the optimization was performed at successively higher resolutions (N = 11, 21, and 41), with each optimization providing an initial guess for the next, with a small amount of noise added to avoid local minima. We found no qualitative difference in the resulting forces other than resolution when N was varied from 11 to 41, all results are shown with N = 41.

The human data are from two subjects, one walking, one running. We believe these data to be representative of previously published data (e.g. [27, 33]).

BIBLIOGRAPHY

[1] Peter G. Adamczyk, Steven H. Collins, and Arthur D. Kuo. The advantages of a rolling foot in human walking. *Journal of Experimental Biology*, 209(20):3953–3963, October 2006. PMID: 17023589.

[2] Peter G. Adamczyk and Arthur D. Kuo. Redirection of center-of-mass velocity during the step-to-step transition of human walking. *Journal of Experimental Biology*, 212(16):2668–2678, August 2009. PMID: 19648412.

[3] R. M. Alexander. Energy-saving mechanisms in walking and running. *Journal of Experimental Biology*, 160(1):55–69, October 1991. PMID: 1960518.

[4] R. McN Alexander. Three uses for springs in legged locomotion. *The International Journal of Robotics Research*, 9(2):53–61, April 1990.

[5] J. C. Alvarez, R. C. Gonzalez, D. Alvarez, and A. M. Lopez. Multisensor Approach to Walking Distance Estimation with Foot Inertial Sensing. In *Proceedings of the Engineering in Medicine and Biology Society*, pages 5719–5722, Lyon, France, August 2007.

[6] R. O. Andres and S. K. Stimmel. Prosthetic alignment effects on gait symmetry: a case study. *Clinical Biomechanics*, 5(2):88–96, May 1990.

[7] C. J. Barclay, R. C. Woledge, and N. A. Curtin. Energy turnover for ca2+ cycling in skeletal muscle. *Journal of Muscle Research and Cell Motility*, 28(4-5):259–274, April 2007.

[8] Catherine E. Bauby and Arthur D. Kuo. Active control of lateral balance in human walking. *Journal of Biomechanics*, 33(11):1433–1440, November 2000.

[9] M. Bergstrom and E. Hultman. Energy cost and fatigue during intermittent electrical stimulation of human skeletal muscle. *Journal of Applied Physiology*, 65(4):1500–1505, October 1988. PMID: 3182513.

[10] Lindsay J. Bhargava, Marcus G. Pandy, and Frank C. Anderson. A phenomenological model for estimating metabolic energy consumption in muscle contraction. *Journal of Biomechanics*, 37(1):81–88, January 2004.

[11] Johann Borenstein and Lauro Ojeda. Heuristic drift elimination for personnel tracking systems. *Journal of Navigation*, 63(04):591–606, September 2010.

[12] Johann Borenstein and Lauro Ojeda. Heuristic drift elimination for personnel tracking systems. *Journal of Navigation*, 63(04):591–606, September 2010.

[13] Jennifer S Brach, Jaime E Berlin, Jessie M VanSwearingen, Anne B Newman, and Stephanie A Studenski. Too much or too little step width variability is associated with a fall history in older persons who walk at or near normal gait speed. *Journal of NeuroEngineering and Rehabilitation*, 2:21, July 2005. PMID: 16042812 PMCID: PMC1187917.

[14] Jennifer S. Brach, Jaime E. Berlin, Jessie M. VanSwearingen, Anne B. Newman, and Stephanie A. Studenski. Too much or too little step width variability is associated with a fall history in older persons who walk at or near normal gait speed. *Journal of neuroengineering and rehabilitation*, 2:21, 2005.

[15] J M Brockway. Derivation of formulae used to calculate energy expenditure in man. *Human nutrition. Clinical nutrition*, 41(6):463–471, November 1987. PMID: 3429265.

[16] Mon S Bryant, Diana H Rintala, Jyhgong G Hou, Ann L Charness, Angel L Fernandez, Robert L Collins, Jeff Baker, Eugene C Lai, and Elizabeth J Protas. Gait variability in parkinson's disease: influence of walking speed and dopaminergic treatment. *Neurological research*, 33(9):959–964, November 2011.

[17] Arthur E. Bryson. *Applied Linear Optimal Control: Examples and Algorithms*. Cambridge University Press, August 2002.

[18] G. A. Cavagna, F. P. Saibene, and R. Margaria. External work in walking. *Journal of Applied Physiology*, 18(1):1–9, January 1963. PMID: 14019429.

[19] Steven H. Collins, Peter G. Adamczyk, and Arthur D. Kuo. Dynamic arm swinging in human walking. *Proceedings of the Royal Society B: Biological Sciences*, 276(1673):3679–3688, October 2009. PMID: 19640879.

[20] Roy D. Crowninshield and Richard A. Brand. A physiologically based criterion of muscle force prediction in locomotion. *Journal of Biomechanics*, 14(11):793–801, 1981.

[21] K L Davie, J E Oram Cardy, J D Holmes, M Gagnon, A Hyde, M E Jenkins, and A M Johnson. The effects of word length, articulation, oral-motor movement, and lexicality on gait: a pilot study. *Gait and posture*, 35(4):691–693, April 2012.

[22] Kristin V Day, Steven A Kautz, Samuel S Wu, Sarah P Suter, and Andrea L Behrman. Foot placement variability as a walking balance mechanism post-spinal cord injury. *Clinical biomechanics*, 27(2):145–150, February 2012.

[23] Jesse C. Dean and Arthur D. Kuo. Energetic costs of producing muscle work and force in a cyclical human bouncing task. *Journal of Applied Physiology*, 110(4):873–880, April 2011.

[24] J. Doke and A. D. Kuo. Energetic cost of producing cyclic muscle force, rather than work, to swing the human leg. *Journal of Experimental Biology*, 210(13):2390–2398, July 2007.

[25] Jiro Doke, J. Maxwell Donelan, and Arthur D. Kuo. Mechanics and energetics of swinging the human leg. *The Journal of Experimental Biology*, 208(3):439–445, February 2005. PMID: 15671332.

[26] J M Donelan, R Kram, and A D Kuo. Mechanical and metabolic determinants of the preferred step width in human walking. *Proceedings. Biological sciences / The Royal Society*, 268(1480):1985–1992, October 2001. PMID: 11571044 PMCID: PMC1088839.

[27] J Maxwell Donelan, Rodger Kram, and Arthur D Kuo. Mechanical work for step-to-step transitions is a major determinant of the metabolic cost of human walking. *The Journal of Experimental Biology*, 205(Pt 23):3717–3727, December 2002. PMID: 12409498.

[28] J. Maxwell Donelan, David W. Shipman, Rodger Kram, and Arthur D. Kuo. Mechanical and metabolic requirements for active lateral stabilization in human walking. *Journal of Biomechanics*, 37(6):827–835, June 2004. PMID: 15111070.

[29] J.Maxwell Donelan, Rodger Kram, and Arthur D. Kuo. Simultaneous positive and negative external mechanical work in human walking. *Journal of Biomechanics*, 35(1):117–124, January 2002.

[30] P. Esser, H. Dawes, J. Collett, M. G. Feltham, and K. Howells. Assessment of spatio-temporal gait parameters using inertial measurement units in neurological populations. *Gait and Posture*, 34(4):558–560, Oct 2011.

[31] E. Foxlin. Pedestrian tracking with shoe-mounted inertial sensors. *IEEE Computer Graphics and Applications*, 25(6):38–46, 2005.

[32] T. Fukunaga, K. Kubo, Y. Kawakami, S. Fukashiro, H. Kanehisa, and C. N. Maganaris. In vivo behaviour of human muscle tendon during walking. *Proceedings of the Royal Society B: Biological Sciences*, 268(1464):229–233, February 2001. PMID: 11217891 PMCID: PMC1088596.

[33] Hartmut Geyer, Andre Seyfarth, and Reinhard Blickhan. Compliant leg behaviour explains basic dynamics of walking and running. *Proceedings of the Royal Society B: Biological Sciences*, 273(1603):2861–2867, November 2006. PMID: 17015312 PMCID: PMC1664632.

[34] Stanton A. Glantz. *Primer of Biostatistics: Sixth Edition*. McGraw Hill Professional, April 2005.

[35] Keith E. Gordon, Daniel P. Ferris, and Arthur D. Kuo. Metabolic and mechanical energy costs of reducing vertical center of mass movement during gait. *Archives of Physical Medicine and Rehabilitation*, 90(1):136–144, January 2009.

[36] Mark D Grabiner and Karen L Troy. Attention demanding tasks during treadmill walking reduce step width variability in young adults. *Journal of Neuroengineering and Rehabilitation*, 2:25, 2005.

[37] D. W. Grieve and Ruth J. Gear. The relationships between length of stride, step frequency, time of swing and speed of walking for children and adults. *Ergonomics*, 9(5):379–399, 1966.

[38] Christopher M. Harris and Daniel M. Wolpert. Signal-dependent noise determines motor planning. *Nature*, 394(6695):780–784, August 1998.

[39] N. C. Heglund, M. A. Fedak, C. R. Taylor, and G. A. Cavagna. Energetics and mechanics of terrestrial locomotion. IV. total mechanical energy changes as a function of speed and body size in birds and mammals. *Journal of Experimental Biology*, 97(1):57–66, April 1982. PMID: 7086351.

[40] Russell T Hepple, Richard A Howlett, Casey A Kindig, Creed M Stary, and Michael C Hogan. The o2 cost of the tension-time integral in isolated single myocytes during fatigue. *American journal of physiology. Regulatory, integrative and comparative physiology*, 298(4):R983–988, April 2010. PMID: 20130224 PMCID: PMC2853400.

[41] A L Hof, S M Vermerris, and W A Gjaltema. Balance responses to lateral perturbations in human treadmill walking. *The Journal of Experimental Biology*, 213(Pt 15):2655–2664, August 2010. PMID: 20639427.

[42] Michael C. Hogan, Erica Ingham, and S. Sadi Kurdak. Contraction duration affects metabolic energy cost and fatigue in skeletal muscle. *American Journal of Physiology - Endocrinology And Metabolism*, 274(3):E397–E402, March 1998. PMID: 9530120.

[43] J. Horowitz, L. Sidossis, and E. Coyle. High efficiency of type i muscle fibers improves performance. *International Journal of Sports Medicine*, 15(03):152–157, March 2008.

[44] Michal Katz-Leurer, Hemda Rotem, Ofer Keren, and Shirley Meyer. Effect of concurrent cognitive tasks on gait features among children post-severe traumatic brain injury and typically-developed controls. *Brain injury*, 25(6):581–586, 2011.

[45] K.R. Kaufman, K.-N. An, W.J. Litchy, and E.Y.S. Chao. Physiological prediction of muscle forcesI. theoretical formulation. *Neuroscience*, 40(3):781–792, 1991.

[46] Amy E. Kerdok, Andrew A. Biewener, Thomas A. McMahon, Peter G. Weyand, and Hugh M. Herr. Energetics and mechanics of human running on surfaces of different stiffnesses. *Journal of Applied Physiology*, 92(2):469–478, February 2002. PMID: 11796653.

[47] A. Kose, A. Cereatti, and U. D. Croce. Estimation of traversed distance in level walking using a single inertial measurement unit attached to the waist. In *Proceedings of the IEEE Engineering in Medicine & Biology Society*, pages 1125–1128, 2011.

[48] Rodger Kram and C. Richard Taylor. Energetics of running: a new perspective. *Nature*, 346(6281):265–267, July 1990.

[49] Arthur D. Kuo. Stabilization of lateral motion in passive dynamic walking. *The International Journal of Robotics Research*, 18(9):917–930, September 1999.

[50] Arthur D. Kuo. A simple model of bipedal walking predicts the preferred SpeedStep length relationship. *Journal of Biomechanical Engineering*, 123(3):264, 2001.

[51] Arthur D. Kuo. The six determinants of gait and the inverted pendulum analogy: A dynamic walking perspective. *Human Movement Science*, 26(4):617–656, August 2007.

[52] Arthur D. Kuo and J. Maxwell Donelan. Dynamic principles of gait and their clinical implications. *Physical Therapy*, 90(2):157–174, February 2010. PMID: 20023002.

[53] Arthur D Kuo, J Maxwell Donelan, and Andy Ruina. Energetic consequences of walking like an inverted pendulum: step-to-step transitions. *Exercise and Sport Sciences Reviews*, 33(2):88–97, April 2005. PMID: 15821430.

[54] Q. Li, M. Young, V. Naing, and J. M. Donelan. Walking speed estimation using a shank-mounted inertial measurement unit. *Journal of Biomechanics*, 43(8):1640–1643, May 2010.

[55] Shiping Ma and George I. Zahalak. A distribution-moment model of energetics in skeletal muscle. *Journal of Biomechanics*, 24(1):21–35, 1991.

[56] B. E. Maki. Gait changes in older adults: predictors of falls or indicators of fear. *Journal of the American Geriatrics Society*, 45(3):313–320, Mar 1997.

[57] Rodolfo Margaria. Positive and negative work performances and their efficiencies in human locomotion. *Internationale Zeitschrift fr angewandte Physiologie einschlielich Arbeitsphysiologie*, 25(4):339–351, December 1968.

[58] B. Mariani, C. Hoskovec, S. Rochat, C. Bula, J. Penders, and K. Aminian. 3D gait assessment in young and elderly subjects using foot-worn inertial sensors. *Journal of Biomechanics*, 43(15):2999–3006, Nov 2010.

[59] MATLAB. *version 7.12.0.635 (R2011a)*. The MathWorks Inc., Natick, Massachusetts, 2011.

[60] Tad McGeer. Passive dynamic walking. *The International Journal of Robotics Research*, 9(2):62–82, April 1990.

[61] Kenneth O. Mcgraw and S. P. Wong. Forming Inferences About Some Intraclass Correlation Coefficients. *Psychological Methods*, 1(1):30–46, March 1996.

[62] T A McMahon and G C Cheng. The mechanics of running: how does stiffness couple with speed? *Journal of biomechanics*, 23 Suppl 1:65–78, 1990. PMID: 2081746.

[63] J. P. Meijaard, Jim M. Papadopoulos, Andy Ruina, and A. L. Schwab. Linearized dynamics equations for the balance and steer of a bicycle: a benchmark and review. *Proceedings of the Royal Society A: Mathematical, Physical and Engineering Science*, 463(2084):1955–1982, August 2007.

[64] William C. Miller, Mark Speechley, and Barry Deathe. The prevalence and risk factors of falling and fear of falling among lower extremity amputees. *Archives of Physical Medicine and Rehabilitation*, 82(8):1031–1037, August 2001.

[65] A. E. Minetti and R. McN Alexander. A theory of metabolic costs for bipedal gaits. *Journal of Theoretical Biology*, 186(4):467 – 476, 1997.

[66] R R Neptune and S A Kautz. Muscle activation and deactivation dynamics: the governing properties in fast cyclical human movement performance? *Exercise and sport sciences reviews*, 29(2):76–80, April 2001. PMID: 11337827.

[67] Shawn M. OConnor, Henry Z. Xu, and Arthur D. Kuo. Energetic cost of walking with increased step variability. *Gait & Posture*, 36(1):102–107, May 2012.

[68] Lauro Ojeda and Johann Borenstein. Non-gps navigation for security personnel and first responders. *The Journal of Navigation*, 60(03):391–407, 2007.

[69] Lauro Ojeda, John R. Rebula, Peter G. Adamczyk, and Arthur D. Kuo. Mobile platform for motion capture of locomotion over long distances. *Journal of Biomechanics*, 46(13):2316 – 2319, 2013.

[70] T. M. Owings and M. D. Grabiner. Step width variability, but not step length variability or step time variability, discriminates gait of healthy young and older adults during treadmill locomotion. *Journal of Biomechanics*, 37(6):935–938, Jun 2004.

[71] Tammy M Owings and Mark D Grabiner. Measuring step kinematic variability on an instrumented treadmill: how many steps are enough? *Journal of biomechanics*, 36(8):1215–1218, August 2003.

[72] John R. Rebula, Lauro V. Ojeda, Peter G. Adamczyk, and Arthur D. Kuo. Measurement of foot placement and its variability with inertial sensors. *Gait & Posture*, 38(4):974–980, September 2013.

[73] Noah J. Rosenblatt and Mark D. Grabiner. Measures of frontal plane stability during treadmill and overground walking. *Gait & Posture*, 31(3):380–384, March 2010.

[74] Andy Ruina, John E A Bertram, and Manoj Srinivasan. A collisional model of the energetic cost of support work qualitatively explains leg sequencing in walking and galloping, pseudo-elastic leg behavior in running and the walk-to-run transition. *Journal of theoretical biology*, 237(2):170–192, November 2005. PMID: 15961114.

[75] A. M. Sabatini, C. Martelloni, S. Scapellato, and F. Cavallo. Assessment of walking features from foot inertial sensing. *IEEE Transactions on Biomedical Engineering*, 52(3):486–494, Mar 2005.

[76] J. B. dec. M. Saunders, Verne T. Inman, and Howard D. Eberhart. The major determinants in normal and pathological gait. *The Journal of Bone & Joint Surgery*, 35(3):543–558, July 1953.

[77] H. Martin Schepers, Edwin H.F. van Asseldonk, Chris T.M. Baten, and Peter H. Veltink. Ambulatory estimation of foot placement during walking using inertial sensors. *Journal of Biomechanics*, 43(16):3138 – 3143, 2010.

[78] Mariano Serrao, Francesco Pierelli, Alberto Ranavolo, Francesco Draicchio, Carmela Conte, Romildo Don, Roberto Di Fabio, Margherita LeRose, Luca Padua, Giorgio Sandrini, and Carlo Casali. Gait pattern in inherited cerebellar ataxias. *Cerebellum*, 11(1):194–211, March 2012.

[79] Hiroyuki Shimada, Kenji Ishii, Kiichi Ishiwata, Keiichi Oda, Megumi Suzukawa, Hyuma Makizako, Takehiko Doi, and Takao Suzuki. Gait adaptability and brain activity during unaccustomed treadmill walking in healthy elderly females. *Gait and Posture*, December 2012.

[80] Stale Skogstad, Kristian Nymoen, Yago de Quay, and Alexander Refsum Jensenius. Osc implementation and evaluation of the xsens mvn suit. In *Proceedings of the International Conference on New Interfaces for Musical Expression*, pages 300–303, Oslo, Norway, 2011. The University of Oslo.

[81] Michael J Socie, Robert W Motl, John H Pula, Brian M Sandroff, and Jacob J Sosnoff. Gait variability and disability in multiple sclerosis. *Gait and posture*, November 2012.

[82] L. M. Sonneborn and F. S. Van Vleck. The bang-bang principle for linear control systems. *Journal of the Society for Industrial and Applied Mathematics Series A Control*, 2(2):151–159, January 1964.

[83] Manoj Srinivasan and Andy Ruina. Computer optimization of a minimal biped model discovers walking and running. *Nature*, 439(7072):72–75, September 2005.

[84] S Strogatz. *Nonlinear dynamics and chaos: with applications to physics, biology, chemistry and engineering*. Perseus Books Group, 2001.

[85] Darryl G Thelen. Adjustment of muscle mechanics model parameters to simulate dynamic contractions in older adults. *Journal of biomechanical engineering*, 125(1):70–77, February 2003. PMID: 12661198.

[86] Darryl G. Thelen, Frank C. Anderson, and Scott L. Delp. Generating dynamic simulations of movement using computed muscle control. *Journal of Biomechanics*, 36(3):321–328, March 2003.

[87] Brian R Umberger, Karin G M Gerritsen, and Philip E Martin. A model of human muscle energy expenditure. *Computer methods in biomechanics and biomedical engineering*, 6(2):99–111, April 2003. PMID: 12745424.

[88] Brian R. Umberger, Karin G. M. Gerritsen, and Philip E. Martin. Muscle fiber type effects on energetically optimal cadences in cycling. *Journal of Biomechanics*, 39(8):1472–1479, 2006.

[89] A. J. Van Soest and L. J. Richard Casius. Which factors determine the optimal pedaling rate in sprint cycling?:. *Medicine & Science in Sports & Exercise*, 32(11):1927–1934, November 2000.

[90] Jack M. Wang, Samuel R. Hamner, Scott L. Delp, and Vladlen Koltun. Optimizing locomotion controllers using biologically-based actuators and objectives. *ACM Transactions on Graphics*, 31(4):25:125:11, July 2012.

[91] Robert L. Waters and Sara Mulroy. The energy expenditure of normal and pathologic gait. *Gait & Posture*, 9(3):207–231, July 1999.

[92] E. R. Westervelt, J.W. Grizzle, and D.E. Koditschek. Hybrid zero dynamics of planar biped walkers. *IEEE Transactions on Automatic Control*, 48(1):42–56, January 2003.

[93] Michael W Whittle. Generation and attenuation of transient impulsive forces beneath the foot: a review. *Gait & Posture*, 10(3):264–275, December 1999.

[94] David A Winter. *Biomechanics and motor control of human movement*. Wiley, Hoboken, N.J., 2009.

[95] M. Wisse. Skateboards, bicycles, and three-dimensional biped walking machines: Velocity-dependent stability by means of lean-to-yaw coupling. *The International Journal of Robotics Research*, 24(6):417–429, June 2005.

[96] G I Zahalak and S P Ma. Muscle activation and contraction: constitutive relations based directly on cross-bridge kinetics. *Journal of biomechanical engineering*, 112(1):52–62, February 1990. PMID: 2308304.

[97] G I Zahalak and I Motabarzadeh. A re-examination of calcium activation in the huxley cross-bridge model. *Journal of biomechanical engineering*, 119(1):20–29, February 1997. PMID: 9083845.

[98] C. Zampieri, A. Salarian, P. Carlson-Kuhta, K. Aminian, J. G. Nutt, and F. B. Horak. The instrumented timed up and go test: potential outcome measure for disease modifying therapies in Parkinson's disease. *Journal of Neurology, Neurosurgery and Psychiatry*, 81(2):171–176, Feb 2010.

[99] Karl E. Zelik and Arthur D. Kuo. Human walking isn't all hard work: evidence of soft tissue contributions to energy dissipation and return. *The Journal of Experimental Biology*, 213(24):4257–4264, December 2010. PMID: 21113007.

[100] Karl E. Zelik and Arthur D. Kuo. Mechanical work as an indirect measure of subjective costs influencing human movement. *PLoS ONE*, 7(2):e31143, February 2012.

[101] W. Zijlstra and A. L. Hof. Assessment of spatio-temporal gait parameters from trunk accelerations during human walking. *Gait and Posture*, 18(2):1–10, Oct 2003.